2013-01-01

Identification Of Chemotherapeutic Agents Against Leishmaniasis And Chagas' Disease

Miguel Abran Vasquez
University of Texas at El Paso, mavasquez2@miners.utep.edu

IDENTIFICATION OF CHEMOTHERAPEUTIC AGENTS AGAINST LEISHMANIASIS AND CHAGAS' DISEASE

MIGUEL ABRAN VASQUEZ

Department of Biological Sciences

APPROVED:

Rosa A. Maldonado, D.Sc., Chair

Robert A. Kirken, Ph.D.

Siddartha Das, Ph.D

Igor C. Almeida, D.Sc.

Rodrigo X. Armijos, M.D.,Ph.D.

Benjamin C. Flores, Ph.D.
Dean of the Graduate School

Dedication

I dedicate this work to my family and my biggest supporter, my wife. I dedicate this to my wife for always being there for me throughout all of the hard work and stress that comes with process of research and graduate school and I love her dearly for that. She not only supported me in every way imaginable but she gave me the courage and confidence to conquer all obstacles that showed up in our path. I also dedicate this to my dad for always encouraging me to focus on getting an education and motivating me to get good grades since I was in elementary school. He also was a constant reminder for me to never forget the most important thing in life, our relationship with god. Without god I do not know what I would have done as it was him that led me in this path that has only brought me to happiness and no regrets. I also would like to dedicate this to my mom for helping to raise me into the person that I am today and for always being there to offer herself and her time in a moment of need. Thank you all.

IDENTIFICATION OF CHEMOTHERAPEUTIC AGENTS AGAINST LEISHMANIASIS AND CHAGAS' DISEASE

by

MIGUEL ABRAN VASQUEZ, B.Sc.

DISSERTATION

Presented to the Faculty of the Graduate School of

The University of Texas at El Paso

in Partial Fulfillment

of the Requirements

for the Degree of

DOCTOR OF PHILOSOPHY

Department of Biological Sciences

THE UNIVERSITY OF TEXAS AT EL PASO

May 2013

Acknowledgements

This study was supported by grant # 2S06GM00812-37 from the NIH/MBRS/NIGMS/SCORE Program. MAV was supported by RISE (5R25GM069621-06) Graduate Research Program. We are thankful to the Biomolecule Analysis Core Facility (BACF), High-throughput Core Facility (HTSCF) and Statistical Consulting Laboratory (SCL) at the Border Biomedical Research Center (BBRC), UTEP, supported by NIH/NCRR grant # 5G12RR008124. We thank Kelly Robinson for providing the Luciferase-expressing *L. major* parasites supported by NIH grant AI29646 to SMB. We are also very grateful for the animal training on the mouse model for leishmaniasis that was provided by Dr. Stephen M. Beverley and Dr. Matt Kuhlman at Washington University in St. Louis. The Canadian Institutes of Health Research are thanked for providing a grant to J.R. Dimmock. Dr. Aguilera, Dr. Carolina Lema, and Dr. Armando Varela are greatly appreciated for bringing the compound library to the BBRC and for providing the training for the BD imaging and flow cytometry experiments. We would also like to thank Enamine for the generation of the PPDK inhibitors library. Alfredo Ornelas, Dr. Michaels, and Emma Arigi are also greatly appreciated for there help on determining the purity of our compounds through NMR and Mass-spec analysis. Moreover, most of this work would not have been possible without the contributions and guidance of committee members Dr. Robert A. Kirken, Dr. Siddhartha Das, Dr. Igor C. Almeida, and Dr. Rodrigo X. Armijos.

Abstract

Patients with clinical manifestations of leishmaniasis and Chagas' disease rely on few drugs that have limited efficacy and considerable side effects. Expanding the diversity of available chemotherapeutic drugs for these diseases is of extreme medical importance. Enones or α,β-unsaturated ketones, initially developed as anti-cancer agents, are a worthy of class of compounds to test for activity against *Leishmania major* and *Trypanosoma cruzi* as these eukaryotic parasites share many of the characteristics exhibited by cancer cells. The anti-parasitic activity of a library of α,β-unsaturated ketones (136 derivatives) was screened against *L. major* as well as in mammalian cells. Three compounds (NC901, NC884, and NC2459) showed high leishmanicidal activity (EC_{50} = 456 nM, 1122 nM, and 20 nM, respectively), without mammalian cell toxicity, and were also highly toxic against. *T. cruzi* epimastigotes (EC_{50} = 468 nM, 475 nM, and 20 nM, respectively). When tested on *in vitro* infections of BALB/c intraperitoneal macrophages or human osteoblasts with metacyclic promastigote and trypomastigote forms of *L. major* and *T. cruzi,* respectively, these three compounds showed strong showed strong inhibition as well (*Lm*-IC_{50} = 1870 nM, 937 nM, and 625 nM; *Tc*-IC_{50} = 301 nM, 987 nM, and 227 nM, respectively) Furthermore, these compounds were shown to be capable of significantly reducing the parasite burden of *L. major* induced cutaneous leishmaniasis *in vivo* with no apparent toxicity in BALB/c mice. Lastly, our experimental results strongly suggested that the mechanism of action of these compounds is through the induction of a mitochondria-dependent apoptosis-like effect in *L. major* promastigotes. These results indicate that enones may be considered as a safe alternative for current chemotherapeutic drugs used to combat leishmaniasis and Chagas' disease.

Table of Contents

List of Tables

List of Figures

Chapter 1: Introduction

Parasitic trypanosomatids cause a variety of diseases, such as leishmaniasis and Chagas disease (CD). *Leishmania* species and *Trypanosoma cruzi* are directly responsible for these diseases, respectively.

1.1 Leishmaniasis

Leishmania spp. are eukaryotic flagellated organisms that can cause a broad spectrum of diseases, depending on the species. Cutaneous leishmaniasis (CL), caused by *Leishmania major*, is the most common form. This form affects the skin and mucous membranes. Skin sores develop and resemble those found in other diseases including tuberculosis, syphilis, leprosy, skin cancer, and fungal infections which cause pain and disfigurement (1). This disease can produce a large number of lesions, sometimes up to 200, causing serious disability and invariably leaving the patient permanently scarred, a stigma that can cause serious social prejudice (1). Approximately 5-10% of CL cases may develop into mucocutaneous leishmaniasis (MCL), in which the parasite disseminates to the nasopharyngeal areas of the face. These destructive metastatic lesions are a result of a hyper-inflammatory immune response against the parasite (2). Visceral leishmaniasis, commonly known as 'kala azar' in the Eastern Hemisphere, is a more severe form in which the parasites migrate and accumulate in vital organs such as the spleen. This form usually leads to deadly complications because the parasite damages the immune system by decreasing the number of disease-fighting cells (3). Approximately 350 million people are at risk of contracting leishmaniasis in 88 countries around the world. It is endemic in nearly half of the globe affecting Latin and South America, Africa, Europe, and Asia. Although leishmaniasis is considered to be a tropical disease, it has now become an emerging concern for the United States as well. Due to the constant deployment of U.S. troops into and out of these endemic regions, approximately 2,500 troops have been diagnosed with leishmaniasis as of 2007 (4). This number continues to increase

and does not take into account the number of cases that remain undiagnosed. There are currently 12 million people infected worldwide with an estimated two million new cases reported each year (5). In addition, co-infections with HIV have increased the burden of leishmaniasis in public health, especially areas endemic for leishmaniasis where access to treatment still remains a challenge (2) (3). As the number of co-infections with HIV continues to rise worldwide, the problems caused by leishmaniasis have only become more serious since co-infected patients may be difficult to diagnose, respond poorly to treatment, and repeatedly relapse (6).

Leishmania parasites are transmitted by the phlebotomine sand fly to its mammalian host during a blood meal on the skin. When the insect inserts its proboscis into the skin of the host it injects anti-coagulants in order to effectively draw blood. It is during this process in which the slender promastigote form of the parasite is injected into the blood stream of the host. Once inside of the host, the metacyclic promastigotes invade macrophages, differentiate, and replicate as obligate intracellular amastigotes and can readily survive within the phagolysosome of host phagocytic cells (7). This hijacked phagolysome then becomes known as a parasitiphorous vacuole which provides breeding grounds for the round, non-motile amastigote form of the parasite. Eventually the replicating amastigotes burst from their cellular compartments and move on to infect more macrophages. The life cycle is completed when another sand fly takes a blood meal and ingests a parasitized cell. The amastigotes then transform back into promastigotes in the fly mid-gut and migrate to the proboscis (8) (Figure 1.1).

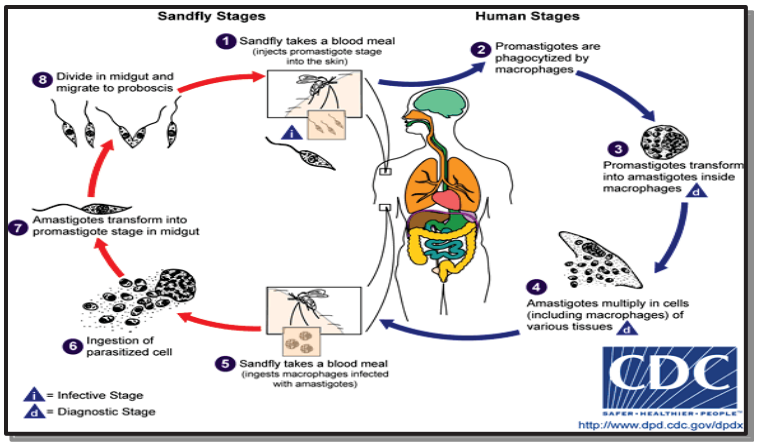

Figure 1.1: Transmission and life cycle of *L. major.* 1. Sandfly takes a blood meal and injects the promastigote form into the skin. 2. Promastigotes are phagocytized by neutrophils and macrophages. 3. Promastigotes transform into amastigotes within the parasitiphorous vacuole of the macrophage. 4. Amastigotes multiply in cells of various tissues through binary fission. 5. The cycle is continued in the insect stage when the sandfly takes a blood meal and ingests macrophages infected with amastigotes. 6. The parasitized cell is ingested and the amastigotes are released. 7. Amastigotes then transform into the promastigote stage in the midgut. 8. The promastigotes are then able to divide in the midgut and migrate to the proboscis where they are ready to be injected into the mammalian host. (9)

Current treatment options for this disease are limited with fungicides and antimony-containing compounds being the only moderately effective drugs available. Pentavalent antimonials remain the most commonly used drugs to treat leishmaniasis in most areas, however in India, drug resistance to antimonials is a major problem (10). Conversely, these compounds require a high dosage for an extended period of time. Unfortunately, toxicity to antimonials increases over time with the development of gastrointestinal symptoms, fever, headache, myalgias, arthralgias, pacreatitis, and rash. In areas where resistance to antimonials is increasing, Miltefosine, a phospholipid disrupting drug, is the first choice of treatment and usually given in combination with liposomal amphotericin B (10). However, drug resistance to these compounds have been widely reported as well and have exhibited many deleterious side effects such as vomiting and diarrhea for Miltefosine and dozens of severe and potentially lethal side effects for amphotericin B that include cardiac, liver, and kidney failure (10) (11).

Lack of specific drugs to treat leishmaniasis has led to a high demand for the availability of newly synthesized therapeutic compounds. Physicians worldwide are clearly in need of higher quality and more diverse treatment options in order to account for the problems posed by the standard treatment options. These facts clearly demonstrate that there is an urgent need for new drugs to treat all forms of leishmaniasis.

1.2 Chagas' Disease

Trypanosoma cruzi, a close genetic relative to species of leishmania, is a eukaryotic haemoflagellate organism that is the etiological agent for Chagas' disease (CD). The pathology of CD can vary greatly; nonetheless, it is usually comprised of three primary stages. Infection with *T. cruzi* begins with a relatively mild acute phase that can resemble the flu or the common cold. If left untreated, the acute phase is followed by a generally long, asymptomatic phase in which the immune system of the host is able to keep the levels of parasitemia at a minimum. Eventually, the disease becomes clinically evident decades after the occurrence of the initial infection affecting up to 40% of the infected individuals in the form of chronic chagasic cardiomyopathy and megasyndrome, or commonly known as the chronic phase of CD (12). This American trypanosome exerts the greatest impact in the Western hemisphere, where estimates of up to 20 million Latin Americans have different forms of CD pathology. Approximately 5 million of these individuals infected with *T. cruzi* are expected to develop severe cardiomyopathy**,** and/or digestive disorders. Regrettably, 50,000 people die every year from these complications (13) (14). Although this disease is not considered to be endemic to the United States, it is becoming an emerging concern for the U.S. as well. The CDC estimates that there are as many as 300,000 individuals in the U.S.

living with *T. cruzi* infection, with that number expected to rise each year due to increasing immigration from endemic areas (15).

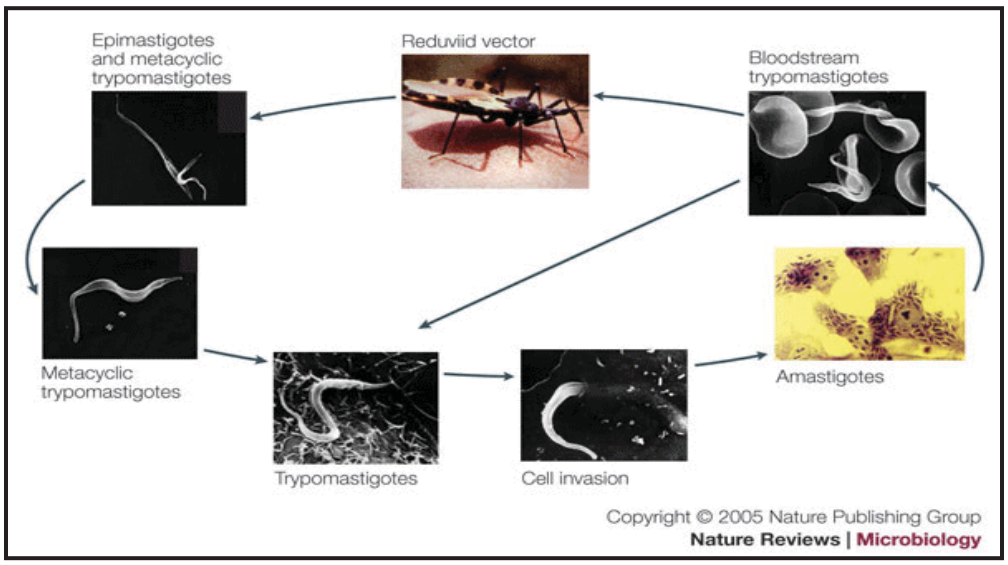

Figure 1.2: Life cycle of *T. cruzi.* First, the reduviid bug takes a blood meal on the mammalian host and defecates simultaneously. The trypomastigote form present in the feces enters the bite site or through any open cavity. Metacyclic trypomastigote penetrate various cells inside of which they transform into amastigotes. Amastigotes then replicate through binary fission and then transform back into trypomastigotes until they burst out of the cell and can move on to infect other cells. The insect stage continues when the reduviid bug takes a blood meal and ingests the trypomastigote form. Trypomastigotes transform in epimastigotes and multiply in the midgut of the vector. The epimastigotes transform into metacyclic trypomastigotes and migrate to the hindgut. (13)

Chagas' disease is a complex zoonosis as most mammals can serve as hosts and reservoirs for *T. cruzi* infection and aid in their distribution of the parasites through migration. Humans are naturally infected with *T. cruzi* with the initial bite of an infected triatomine insect, also known as a "kissing bug". Unlike the sandfly, this insect vector sheds the infective form of the parasite, known as metacyclic trypomastigotes, through its feces (16). The introduction of contaminated feces into the bite site or through the mucous membranes such as the eye are the most common ways in which the human host becomes inoculated with *T. cruzi*. Once inside of the host, the metacyclic trypomastigotes invade nearly any type of host cell where they begin to differentiate into

amastigotes. The amastigotes proliferate via binary fission and eventually differentiate back into trypomastigotes until they burst from the cell, becoming free in the blood targeting other cells for invasion, thus continuing the infective cycle (17). Once released into the blood the trypomastigotes can be transmitted back into the kissing bug through a blood meal, in which the parasite transforms back into an epimastigote within the insect's gut (17). The epimastigotes travel to the hind-gut of the insect, and eventually differentiate into infective metacyclic trypomastigotes to complete the life cycle of *T. cruzi* (Figure 1.2). The transmission of the parasite is usually from the insect vector (80%-90%); however, it is known to be transmitted through other routes, such as contaminated blood transfusions (5-20%), organ transplant, and congenital transmission (0.5-8%) (18).

The current treatment for *T. cruzi* consists of two nitroheterocyclic derivatives, benznidazole and nifurtimox (19). These drugs were developed empirically in the 1960s and 1970s and are very effective in treating the acute stage of the disease, but have limited activity in the chronic (20). Moreover, these compounds have severe side effects including development of invasive lymphomas which has been reported in rabbits (21). Nifurtimox side effects include gastrointestinal and neurological symptoms while benznidazole side effects include granulocytopenia, rash, and peripheral neuropathy (10). In addition, the course of treatment can last from one to four months, and in many cases resulting in incomplete drug schedules, which leads to the development of resistance (22). These facts clearly point out the urgent need for new drugs to treat Chagas' disease.

1.3 Trypanothione Metabolism and Lipoamide Dehydrogenase

Trypanosomatids differ from all other known eukaryotes and prokaryotes in their specific redox system. In contrast to nearly all other organisms they lack glutathione reductase (GR) but have a trypanothione reductase (TR) instead. This makes TR the primary enzyme responsible for

counter-acting oxidative stress as well as many other important functions (23). The basis of the redox system consists of the flavoenzyme trypanothione reductase and the thiol-polyamine conjugate trypanothione (N^1,N^8-bis(glutathionyl)spermidine) (24). The essentiality of this system has been deemed paramount through well established studies as it is responsible for various vital functions within the parasite (25). The reduced form of trypanothione ($T(SH)_2$) is the primary molecule involved in many pathways that require direct reductions that allow many important reactions to proceed (Figure 1.3). The reduction of disulfides, neutralization of free radicals and reactive oxygen species (ROS), detoxification and exportation of metals and drugs, as well as the synthesis of deoxyribonucleotides are just a few of the essential pathways that require the action of trypanothione. This reactive molecule must be kept in the reduced dithiol state in order to be functional in these pathways and is maintained in this form by trypanothione reductase. Trypanosomatids contain a similar acting molecule known as glutathione as well; however, it has shown to be much less reactive than trypanothione. Many spontaneous reactions that surface with trypanothione do not do so with glutathione, such as the reduction of ribonucleotide reductase (25). Also, one crucial difference between the two is that trypanothione is kinetically favored as a reductant of disulfides, another example of how trypanothione dominates the redox cycle in trypanosomes (25).

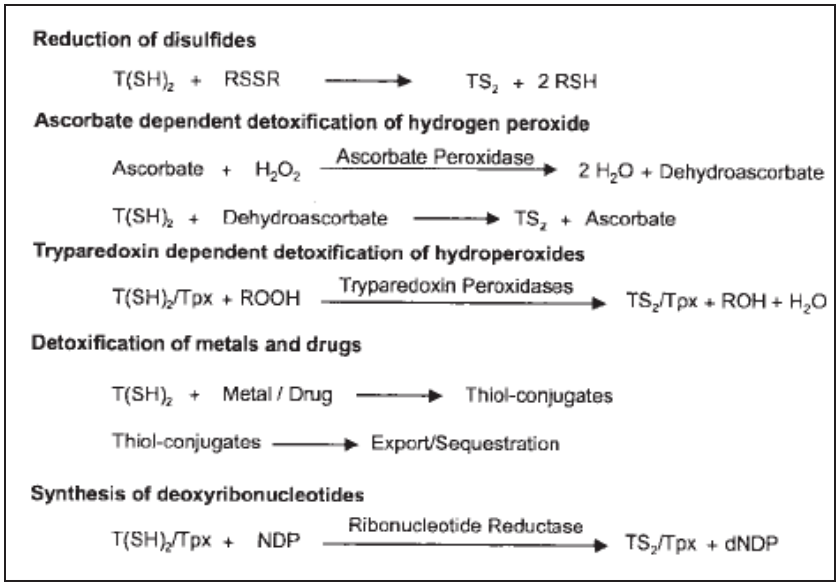

Figure 1.3: Trypanothione-dependent pathways within the parasite. Different disulfides (RSSR) sucha as glutathione are directly reduced by trypanothione to the respective thiols (RSH). Trypanothione ($T(SH)_2$) is involved in the detoxification of hydroperoxides, metals and drugs as well as the synthesis of DNA precursors. At millimolar concentrations, the dithiol also spontaneously reduces hydroperoxides as well as ribonucleotide reductase. Abbreviations: NDP, nucleoside diphosphate; dNDP, deoxynucleoside diphosphate; Tpx, tryparedoxins; TS_2, trypanothione disulfide. (25)

Trypanothione does indeed seem to have taken over most of the classic roles of glutathione, although glutathione is essential for the biosynthesis of trypanothione as it is combined with spermidine by trypanothione synthetase in the final step of the pathway resulting in trypanothione as the product (Figure 1.4) (25). Many of the genes involved in this pathway have been described to be essential in organisms such as leishmania are also up-regulated in drug-resistant mutants as well (25) (26). Overall, it is important to acknowledge that the sensitivity of trypanosomatids towards oxidative stress and the absence of this pathway from the mammalian host render the enzymes of trypanothione metabolism attractive molecules for chemotherapeutic target. Discovering new inhibitors that target this pathway is vital.

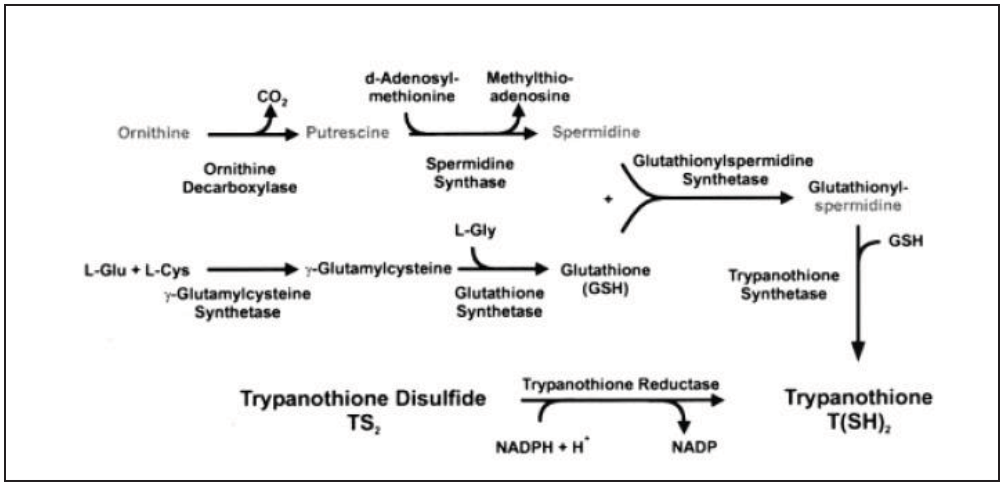

Figure 1.4: Trypanothione biosynthesis. The two components of trypanothione, spermidine (grey) and glutathione (black), are synthesized separately. Subsequently two molecules of glutathione are conjugated with spermidine. Trypanothione disulfide is reduced by trypanothione reductase at the expense of NADPH. (25)

Lipoamide dehydrogenase (LADH) is another flavoenzyme, structurally and mechanistically closely related to TR and GR, and all belong to the family of FAD-disulfide oxidoreductases (27). These complexes play an important role in *T. cruzi* oxidative metabolism through all stages of the parasite. Similar to how TR keeps trypanothione in a reduced state, LADH reversibly catalyses the NADH-dependent reduction of lipoamide, $L(S)_2$ to dihydrolipoamide, $L(SH)_2$ (28). LADH is known to function in the mitochondrion which makes it a good candidate as the enzyme responsible for reducing the tryparedoxins (TXNs) which are involved in reducing hydroperoxides present in the mitochondrial matrix. This idea is relevant because it has been shown that TR is not present in the mitochondria of trypanosomes such as *Leishmania infantum* (29). Since trypanothione is regarded as the sole physiological reductant of TXNs, how is this molecule serving its role within the mitochondria without the presence of TR? A study done by Gutierrez-Correa in 2010 showed that the TR and $T(SH)_2$ redox system can be replaced by the dihydrolipoamide dehydrogenase/lipoamide redox system as a TXN electron donor *in vitro* (28). This evidence supports the notion that LADH

may serve other critical functions within the mitochondria on top of its classically known functions involved with the citric acid cycle.

Since TR and LADH are both structurally and mechanistically similar, it comes as no surprise that there are many inhibitors that inhibit both of these enzymes. For example studies done in 2001 by Davioud-Charvet *et al*. and then in 2009 by Maldonado *et al.* described how 1,4-naphthoquinone derivatives were able to subvert both TR and LADH enzymes from *T. cruzi* (23) (30). Moreover, it was demonstrated that phenothiazine (PTZ) metabolites irreversibly inhibited both of these enzymes as well, contributing to the trypanocidal action of PTZ in *T. cruzi* (28). Discovering new compounds that inhibit the activity of one or both of these enzymes may bring about promising new chemotherapeutic drugs that can be used for the treatment of a wide variety of diseases caused by trypanosomatids.

1.4 α,β-Unsaturated Ketones

In the discovery of novel antiparasitic drugs there has been an increasing interest in the similarities between cancer cells and parasites. Some of these similarities include living and multiplying in the same host, independence from exogenous factors, resistance to programmed cell death (apoptosis), the capacity to proliferate rapidly and infinitely, as well as the ability to disseminate especially in immunocompromised individuals (31). With limited progress in the development of a vaccine and an uprise in drug resistant parasites, alternative treatment options for parasitic diseases are in high demand. One way to circumvent the problems with antiparasitic drug discovery and the reluctance of pharmaceutical companies to invest in tropical disease research is to focus on existing drugs used to treat other human diseases (31). Testing anti-cancer agents for their antiparasitic properties ensures existing data on toxicology, pharmacology, and tolerance in mice or

human subjects (31). At the Border Biodmedical Research Center's High Throughput Drug Screening Facility there is an anti-neoplastic drug library, known as Dimmock's library, which is available for use by members of the department. The compounds in this library are known as α,β-unsaturated ketones or thiol alkylators (32). These drugs were designed to react specifically with thiols and not amino or hydroxyl functionalities in order to bereft the genotoxic effects caused by most anticancer drugs (32). These particular properties of the drug library are very interesting since thiol metabolism is an essential and unique pathway to trypanosomatids and most antiparasitic drugs have difficulties with toxicity. In mammals, most forms of α,β-unsaturated ketones are able to exert their cytotoxic action by at least two mechanisms (32). First, there is a facile displacement of the acyl group by thiols such as glutathione (GSH) and cysteine (32). Second, glyoxalase I is inhibited, which is involved in the metabolism of the cytotoxin methylglyoxal (32). The outcome of these reactions has been shown to increase the number of apoptotic cells in apoptosis-resistant human pancreatic adenocarcinoma cells (32). This effect was eliminated if GSH was added to the culture medium (32). By lowering the levels of GSH, tumors have been shown to be sensitized to other anticancer drugs that are rapidly metabolized by GSH (32). Another key characteristic of these compounds are their ability to inhibit the enzyme glutathione *S*-transferase which is important for the detoxification of oxidants, toxins, and xenobiotics (33). Moreover, these compounds have been shown to be well tolerated in rodents (33), which is important in the development of drugs for diseases like leishmaniasis and Chagas' disease.

Overall, the similarity between parasites and cancer cells as well as the characteristics of Dimmock's library makes testing these compounds for their antiparasitic properties interesting. The potential that these compounds may disturb the thiol or trypanothione metabolism of

trypanosomatids makes these compounds promising for their potential to be cytotoxic to all species in the family of trypanosomatidae.

1.5. Pyruvate Phosphate Dikinase (PPDK)

The energetic metabolism of *T. cruzi* and other trypanosomes is not widely understood, but deserves a closer look. All indications point to the conclusion that it is essential for organisms such as *L. major* and *T. cruzi* to bear efficient energy producing processes in order to survive harsh, nutrient-depleted environments such as in the phagolysome of the macrophage or within the gut of an insect. One organelle involved in the energetic metabolism that has captured the interest of many is the glycosome. The glycosome is an organelle that is very similar to the peroxisome, but a few peculiar aspects make it specific to trypanosomatids. It contains within its own single lipid bi-layer envelope the first six to seven enzymes involved in glycolysis, pathways involved in the reoxidation of NADH, fatty acid oxidation, and biosynthetic pyrophosphate (PPi) producing pathways (34)(35) (Figure 1.5). The glycosome is already known to be an essential part of the *T. cruzi* life cycle; however, its function is still not completely understood. There have been many studies performed on this organelle that have shown that it contains proteins and functional enzymes that are not present in vertebrates. According to Concepcion *et al*, a glycosomal enzyme known as pyruvate phosphate dikinase (PPDK) appears as a central enzyme in the metabolism of the glycosome of *T. cruzi* by providing a link between all of the pathways listed above (35). Moreover, this enzyme is not present in vertebrates or higher eukaryotes, which makes it a good target for the design of drugs against trypanosomes.

The reaction catalyzed by PPDK in *T. cruzi* is highly exergonic (-5.2 kcal/mol) in the direction of pyruvate and ATP production making it the only detectable PPi consuming enzyme in

the glycosome (23). Most organisms use pyrophosphatase (PPase) as their primary PPi consuming enzyme, however, there were no detectable levels of PPase in the glycosome of *T. cruzi* in the study performed by Concepcion *et al*. Additionally, the thermodynamics of PPDK are very similar to those of PPase which strengthens the notion that PPDK may indeed be the link that allows all of the glycosomal PPi-producing enzymes to progress with their reactions (35). It is well established that trypanosomatids also contain large amounts of pyrophosphate stores in organelles known as acidocalcisomes that are believed to be energy stores (36). Without the presence of PPase, the glycosomal PPDK would be in charge of hydrolyzing PPi and eliminating toxic PPi at the same time. Also, it would not make sense to have all of the main PPi-producing pathways compartmentalized without the presence of PPDK (36).

A

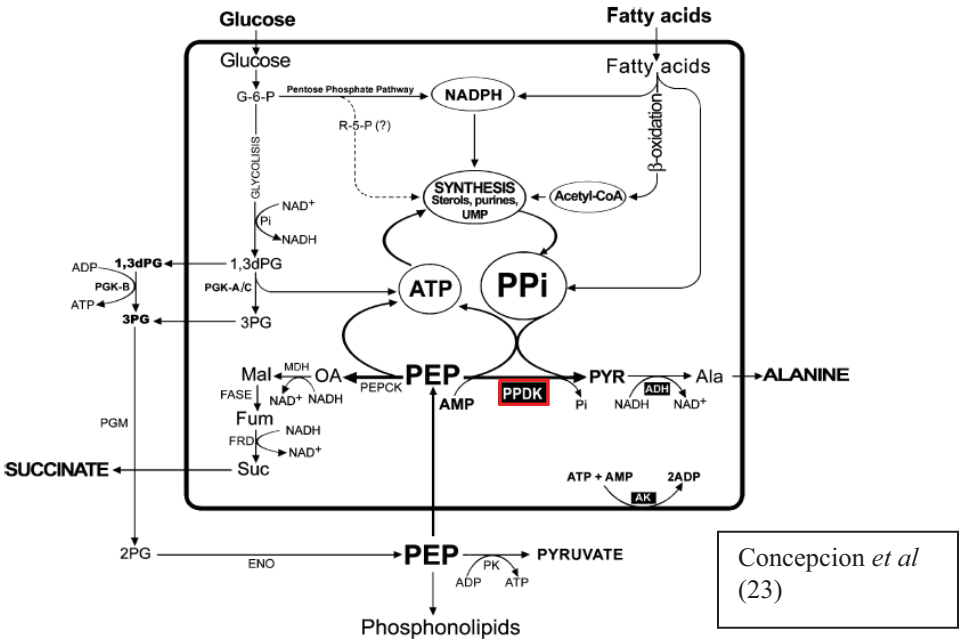

Concepcion *et al* (23)

B

$$PEP + AMP + PPi \underset{PPDK}{\rightleftharpoons} pyruvate + ATP + Pi$$

Figure 1.5: A) A model for the intermediary metabolism of PPi in the glycosomes of *T. cruzi* epimastigotes. All reactions indicated with continuous arrow in this model have been demonstrated in the parasite. B) PPDK catalyzes the reversible reaction of PEP + AMP + pyrophosphate (PPi) to pyruvate + ATP + inorganic phosphate (Pi). Metabolite abbreviations: G-6-P, glucose-6-phosphate; 1.3dPG, 1,3diphosphoglycerate; 3PG, 3phosphoglycerate; 2PG, 2phosphoglycerate; Mal, malate;

OA, oxalacetate; Fum, fumarate; Suc, succinate; PEP, phosphoenolpyruvate; PYR, pyruvate; Ala, alanine. Enzyme abbreviations: PPDK, pyruvate phosphate dikinase; PEPCK, phosphoenolpyruvate carboxykinase; ADH, alanine dehydrogenase; AK, adenylate kinase; MDH, malate dehydrogenase; FASE, fumarase; FRD, fumarate reductase; PGK, phosphoglycerate kinase; PGM, phosphoglycerate mutase; ENO, enolase; PK, pyruvate kinase.

Additionally, the system of PPDK plus alanine dehydrogenase is in charge of maintaining the redox and energy balances of the glycosome. This balance can serve to be an important factor in maintaining the integrity of the glycosome and, in turn, essential for sustaining the viability of the parasite. Interestingly, fatty acid oxidation was reported to be present in the glycosome of *T. cruzi* as well, which is believed to not take place without the hydrolysis of PPi that allows for fatty acids to become activated (35). Another promising finding presented in a study by Maldonado in 2000 is that PPDK does not appear to be developmentally regulated in *T. cruzi* since the protein is detected in all three stages of its life cycle (37). This evidence has contributed to the idea that this enzyme may be essential for many trypanosomes such as *T. cruzi*.

Although pyruvate phosphate dikinase and its precise role within the glycosome are still not widely understood, the evidence stated above makes studying this enzyme for its potential as a chemotherapeutic drug target in more detail vital.

Chapter 2: *In vitro* and *in vivo* evaluation of α,β-unsaturated ketones as anti-trypanosomal agents

2.1 Material and Methods

2.1.1 Synthesis of α,β-unsaturated ketones and preparation of NC library

The synthesis of NC901 and NC884 has been described previously (38). The preparation of NC2459 was achieved by the acylation of 3,5-bis(benzylidene)-4-piperidone with oxalyl chloride (39). The 136 compound library was shipped to the BBRC High-throughput Core Facility (HTSCF) from the University of Saskatchewan in Canada in powdered stocks. The powdered stocks were diluted in DMSO at varying concentrations depending on their solubility in DMSO. Each compound was added to one well in a 96-well plate to be used for drug screening.

2.1.2 Trypanosomatid cultures

Trypomastigote forms of *T. cruzi* Y strain were obtained from infected BALB/c mice by cardiac puncture 4 days following the intraperitoneal infection with 10^5 parasites. The procedure was performed minimizing the distress and pain for the animals following the NIH guidance and animal protocol approved by UTEP's Institutional Animal Care and Use Committee (IACUC). Cell-derived trypomastigotes were initially obtained by infecting Green monkey kidney-derived LLC-MK2 cells (American Type Culture Collection-ATCC, Rockville, MD) as previously described (40). Briefly, semi-confluent host cell monolayers were maintained in DMEM medium (Invitrogen), supplemented with 10% heat-inactivated fetal bovine serum (DMEM-10% FBS), at 37 C, in 5% CO_2 humidified atmosphere. Cells were infected with trypomastigotes at 1:10 host cell/parasite ratio. Four days following the infection, trypomastigotes were harvested from the culture supernatant, centrifuged in 50-ml sterile, endotoxin-free conical polypropylene tubes

(Fisher Scientific) (15 min, 3,000xg, 4 C), washed twice in 5 ml fresh DMEM-10% FBS, resuspended in the same medium, and used in the assays described below. To maintain the trypomastigote virulence, a maximum of nine *in vitro* passages (infections) were performed. The epimastigote forms of *T. cruzi* (Y strain) were grown in liver infusion-tryptose (LIT) medium (41). Mammalian cell-derived trypomastigote forms of *T. cruzi* (Y strain) were obtained from infected LLC-MK2 cells (American Type Culture Collection-ATCC, Manassas, Virginia) monolayers as described (40). Promastigote forms of *L. major* strain Friedlin clone V1 were grown in RPMI 1640 medium (RPMI) supplemented with 30 mM hemin and 10% FBS inactivated and 50 ng/ml streptothricin neosulfate for maintenance of the LUC gene (42).

2.1.3 Culture of mammalian cells

Rhesus monkey kidney epithelial cell LLC-MK2 (American Type Culture Collection-ATCC, Manassas, Virginia # CCL-7), Hs-27 human fibroblasts (American Type Culture Collection-ATCC, Manassas, Virginia), RAW 264.7 murine macrophages (American Type Culture Collection-ATCC, Manassas, Virginia) U2-09 human osteoblasts (American Type Culture Collection-ATCC, Manassas, Virginia # HTB-99) (American Type Culture Collection-ATCC, Manassas, Virginia) cells were cultured in Dulbecco's Modified Eagle's Medium (DMEM), supplemented with 10% inactivated FBS**,** along with 1% of 10,000 units/ml penicillin and 10 mg/ml streptomycin in 0.9% sodium chloride. Intraperitoneal BALB/c mice macrophages were obtained as described (43) and cultured in DMEM high-glucose, +L-glu, supplemented with 10% FBS (inactivated). The procedure was performed minimizing the distress and pain for the

animals following the NIH guidance and animal protocol approved by UTEP's Institutional Animal Care and Use Committee (IACUC).

2.1.4 Evaluation of the NC library activity against *Leishmania major*

The NC library (136 compounds) was screened using firefly luciferase-expressing *L. major* promastigotes referred to as Lmj-FV1-LUC-TK (*L. major* strain Friedlin (MHOM/JL/80/Friedlin) clone V1) engineered to express luciferase following integration of the construct pIR1SAT-LUC(a)-TK(b) (strain B5113) in the rRNA locus (S.M. Hickerson and S.M. Beverley, unpublished data (51) (52)). Enones (stock solutions in DMSO) were diluted (1 nM to 500 μM, in a final 1% DMSO) and added (1 μl per well) to 96-well microplates using an Eppendorf epMotion 5070 automated pipetting system. Promastigotes (10^6/well) were added, and parasite survival was assessed by luciferase activity with the substrate 5′-fluoroluciferin (ONE-Glo Luciferase Assay System, Promega) after 96-h incubation at 28^{o}C, using a luminometer (Luminoskan, Thermo). The bioluminescent intensity was a direct measure of the survival of parasites. This was determined by comparing bioluminescent intensity of *L. major* parasites live/dead with MTT assay and cell counting. The primary compound screens were performed as single wells. The "hit" (positive) were compounds with anti-parasitic activity (<25% inhibition of survival). Only drugs that were non-toxic or with low toxicity to mammalian cells were further investigated, and assayed in triplicate in three independent experiments, the half maximal effective concentrations (EC_{50}) were determined for each drug (44).

2.1.5 Viability assay on mammalian cells and *T. cruzi* epimastigotes

The cytotoxicity and anti-trypanosomal activity of the NC compounds was tested in human Hs27 fibroblasts (ATCC CRL-1634), LLC-MK_2 cells (ATCC CCL-7), RAW 264.7 murine macrophages (ATCC TIB71) (American Type Culture Collection-ATCC, Manassa, Virginia), mice intraperitoneal macrophages and in epimastigote forms of *T. cruzi* Y strain using Alamar Blue assay (Invitrogen - Life Technology, Grand Island, NY). The experiments were performed as described (45) using a range of concentration of 500 μM to 1 nM.

2.1.6 *In vitro* evaluation of the NC drug library on infectivity experiments by high-content imaging assay

Mice intraperitoneal macrophages and human osteoblasts were placed in a microplate and infected with the amastigote forms of *L. major* strain Friedlin clone V1 and *T. cruzi* Y strain respectably, followed by treatment with NC lead compounds [Table 1]. The procedure was performed as previously described (44, 46). Briefly, Image acquisition and analyses of the plates were carried out using the BD Pathway 855 high-resolution fluorescence bioimager system (BD Biosciences). Filter sets appropriate for the excitation and emission spectra of Draq5 were utilized. Images from four fields (3 x 3 montage) were acquired per well with a 20x objective. To perform the host cell segmentation and counting of parasites, the BD AttoVision™ v1.6.2 Sub Object analysis was used. Draq5 creates a background, staining the host cell and parasite nucleus, but defining the cytoplasm as well, determining this way the amount of parasites within each mammalian cell. The host cell nucleus was excluded by size difference. Subsequently, the infection index was calculated based on the mean of these triplicate values by multiplying the

percentage of infected cells and the constraints used in the HCIA assay that was of 2, 3, 5, and 8 parasites per cell (adaptation from Lonardoni et al. 2000 (47).

2.1.7 Mice strains

Female BALB/c mice (6 to 8 week old) were purchased from Harlan Laboratories (Indianapolis, Indiana) and also were bred at UTEP's animal facility. The *in vivo* leishmaniasis experiments were performed minimizing the distress and pain for the animals following the NIH guidance and animal protocol approved by UTEP's Institutional Animal Care and Use Committee (IACUC).

2.1.8 *In vivo* experiments

The *in vivo* experiments were comprised of four groups of five mice each: 1) infected, but not treated [control for the infection - 100 µL of DMSO per day, drug diluent]; 2) treated with NC884, NC901 or NC2459, but not infected with the parasites [control for drug toxicity]; 3) infected with the parasites and treated with amphotericin B (8 mg/kg/day) [reference drug; positive control]; and 4) infected with the parasites and treated with NC884, NC901 or NC2459 [experimental group]. Luciferase expressing metacyclic promastigotes *L. major* (Freidlin V1) were obtained as described previously (43). Suspensions of 1 x 10^5 or 1 x 10^6 parasites per 50 µl of sterile DMEM (endotoxin-free) were injected with a 30G needle into the left hind footpad of BALB/c mice. Two weeks post-infection the compounds were administered once a day by intraperitoneal route, daily for 14 to 17 days. Twice a week, weights were recorded to monitor

toxicity and the thickness of the infected footpad and the non-infected footpad was measured with digital calipers to monitor the progression of the disease. The parasitic load also was evaluated through *in vivo* imaging using luminescence (Kodak Image Station). The mice were injected intra-peritoneally with 150 mg/kg D-luciferin (Sigma, USA) 10 min before imaging, anesthetized with 1-2% isofluorane in oxygen during imaging and the net intensity emitted from the footpad was quantified using the KODAK Image Station software. Parasite burden was expressed as net intensity emitted from *L. major* infected footpad lesions normalized against the background fluorescence of uninfected mice. The presence/absence of parasites was confirmed by PCR using *L. major* methionine aminopeptidase (MetAP1) 1 specific primers: 5'-GGATCCATGCCCTGCGAAGGCTGCGGC-3' and 5'-GAATTCTCAGATTTTGATTTCGCTGGGGTCTTCGG-3' on cDNA reverse transcribed from total RNA extracted from footpad lysate obtained by macerating footpad tissue fragments in Trizol (Invitrogen Life Technologies, United States) with the gentleMACS™ Dissociator (Miltenyi Biotec GmbH, Germany) following the manufacturer's protocol.

2.1.9 Detection of apoptosis-like effect by annexin V assay

Apoptosis was evaluated using Alexa Fluor® 488 Annexin V/PI Apoptosis Kit (Initrogen™-Life technology, Grand Island, NY). *L. major* promastigotes and BALB/c mice intraperitoneal macrophages were treated with each compound for 24 h. After exposure, the parasites (5×10^7) and macrophages (5×10^6) were harvested, washed and resuspended with PBS. The Annexin V/PI staining of cells followed the manufacturer's instructions. Then the samples were analyzed

with Beckman Coulter Fc500 flow cytometer (Beckman Coulter, USA). The results were expressed as the number of annexin positive cells per thousand cells counted.

2.1.10 Polychromatic analysis of mitochondrial membrane potential ($\Delta\psi_m$)

L. major promastigotes and intraperitoneal macrophages from BALB/c mice were treated with each compound at three concentrations for four hours. Then, cells were stained with 2 μM of the fluorophore 5,5',6,6'-tetrachloro-1,1',3,3'-tetraethylbenzimidazolylcarboncyanine iodide (JC-1) following a modified version of manufacturer's instruction (Life Technologies, Grand Island, NY). The disruption of mitochondrial $\boldsymbol{\Delta\psi_m}$ is evidenced by an appreciable shift of the fluorescence signal from red to green. JC-1 aggregates or monomers, emitting red or green signal, were identified *via* flow cytometer (Cytomics Fc500) by using FL-2 or FL-1 detectors, respectively. A proton ionophore that dissipates the mitochondrial $\boldsymbol{\Delta\psi_m}$, carbonyl cyanide 3-chlorophenylhydrazone (CCCP) at 50 μM , was used as a positive control. Cells treated with the diluent of the compounds (DMSO) and untreated were used as negative controls. Data collection and analysis was performed by using CXP software (Beckman Coulter). JC-1 is the most widely applied method for detecting mitochondrial depolarization occurring in the early stages of apoptosis (48).

2.1.11 Trypanothione Reductase Inhibition Assays

TR activity is measured spectrophotometrically as described above. The assay mixture (1 mL) contains 100 μM NADPH and 10-15 mU TR. The enzyme activity is followed at two fixed concentrations of 40 and 110 μM TS_2 in the absence and presence of 100 μM inhibitor. Control

assays containing the respective amount of DMSO are carried out where appropriate. To determine the inhibitor constants the activity of *T. cruzi* TR was followed in the absence and presence of different fixed concentrations of inhibitor varying the TS_2-concentration between 20 and 200 μM. The type of inhibition is derived from Lineweaver-Burk and Dixon plots. The inhibitor constants were either obtained graphically from secondary plots or calculated from the expressions for the slopes and intercepts on the vertical axis of the Lineweaver-Burk plots.

2.1.12 Irreversible Inhibition of Trypanothione Reductase

To monitor a potential time-dependent inactivation, 0.5 μM TR is incubated at 25 °C in the presence and absence of 200 μM NADPH with various concentrations of inhibitor in TR assay buffer (total volume of 100-200 μL). At different time intervals, aliquots of 5 μL are removed and the remaining activity is measured in a standard TR assay. Due to the dilution, reversible inhibition is not recorded under these conditions. As control, TR is incubated with NADPH and the respective amount of DMSO. Under these conditions, DMSO does not affect enzyme activity. A second control contains enzyme and inhibitor but no NADPH. To confirm the irreversible inhibition of TR by a compound, an enzyme sample with < 5% remaining activity is prepared. The low molecular mass components are removed by centrifugation in a Microcon YM-30 centrifugal filter (Sorvall Centrifuge RC-5C, 4 ºC). After repeated rinsing with TR assay buffer, the enzyme solution is recovered and its activity measured in a standard TR assay. In addition, the sample is treated with 3 mM dithioerythritol for 1 h and again the enzyme activity measured.

2.1.13 Lipoamide Dehydrogenase Assay

The inhibition of recombinant LADH by diaryldienones derivates will be measured in 1 ml of 50 mM potassium phosphate, 1 mM EDTA, pH 7.0, at 25 ˚C. The reaction mixture will contain 1 mM NAD, 65 to 520 μM dihydrolipoamide (Boehringer Mannheim, Ingelheim, Germany), and several concentrations of the compounds will be assayed. The reaction will be initiated by the addition of the enzyme, and the absorption increases at 340 nm were followed (43).

2.1.14 Statistical analysis

The statistical significance (p-value) of the compound's cytotoxicity was calculated using the General Linear Mixed Model Analysis. This analysis was used to test the linear effect of the logarithm of dose on the logit transformation of the percent survival. The IC_{50} was obtained as the exponent of the negative ratio of the y-intercept and the slope of the fitted regression line (SAS Software, Version 9.2). The graphs for display were attained using Graph Pad Prism 5 Software (GraphPad Software, Inc., La Jolla, California). All experiments had statistical significance determined at $p \leq 0.05$(*), $p \leq 0.01$(**), and $p \leq 0.001$(***).

2.2 Hypothesis

It is hypothesized that some α,β-unsaturated ketones will exhibit antiparasitic properties through the inhibition of enzymes or molecules involved in the parasite's trypanothione or thiol metabolism.

2.3 Results

2.3.1 *In vitro* evaluation of antiparasitic and cytotoxic effects

In these experiments, the novel NC chemical library of 136 compounds was screened for anti-parasitic and cytotoxic activity to mammalian cells. Compounds were incubated with *Leishmania major* promastigotes or LLC-MK_2 cells for 96 hours and were analyzed for toxicity. As summarized in Figure 2.1, 64 of these compounds effectively inhibited the survival of *L. major* promastigotes by 75% or greater. At the same concentrations 20 compounds displayed minimal to no toxicity (>75% survival) when treated against LLC-MK_2 cells. Out of the 64 and 20 compounds that met our initial criteria, six of these compounds met the criteria for both anti-parasitic activity and cytotoxicity to mammalian cells. These six compounds were then tested in several mammalian cell lines (Figure 2.2). The mammalian cells screened for toxicity were Hs27 human fibroblasts, LLC-MK_2 cells, RAW 264.7 murine macrophages, and BALB/c intraperitoneal macrophages. *L. major* promastigotes were also tested at various concentrations to determine the EC_{50} after 24, 48, 72, and 96 hour treatment periods. After a 96 hour treatment, the estimated EC_{50} calculated using *t*-test and linear regression analysis for compounds NC901, NC884, and NC2459 were 453 nM, 1.12 μM, and 20 nM, respectively (Figure 2.3).

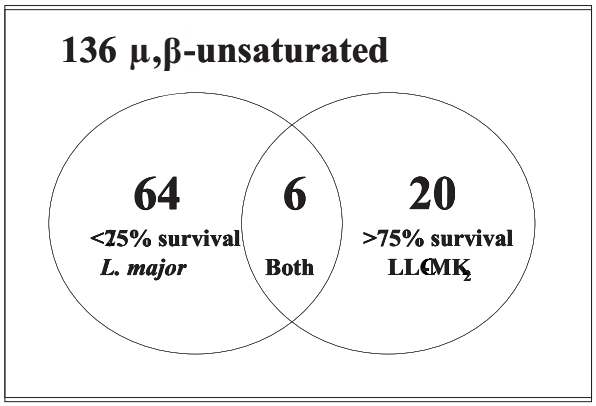

Figure 2.1: Drug screening results and criteria for identifying potential drug candidates. The NC library (Dimmock's library) of 136 compounds was screened for anti-parasitic and cytotoxic activity to mammalian cells (LLC-MK_2). The criteria used to identify potential hits were the observance of less than 25% survival of *L. major* promastigotes and greater than 75% survival in LLC-MK_2 cells. Six compounds met these criteria and additional toxicity assays narrowed down the number of candidate compounds to three.

After evaluating the six compounds in several mammalian cell lines, only three compounds (NC901, NC884 and NC2459) showed a significant difference between the concentrations needed for anti-parasitic activity and cytotoxicity to mammalian cells. All three of these compounds exhibited a 10-fold or greater difference between the EC_{50} of the parasites and the IC_{50} of all three mammalian cell lines with the exception of a 7-fold difference for compound NC884 when treated against murine macrophages (Table 2.1). Remarkably, compound NC2459 showed a minimum of a 100-fold difference between the EC_{50} for the parasites and for all three mammalian cell lines.

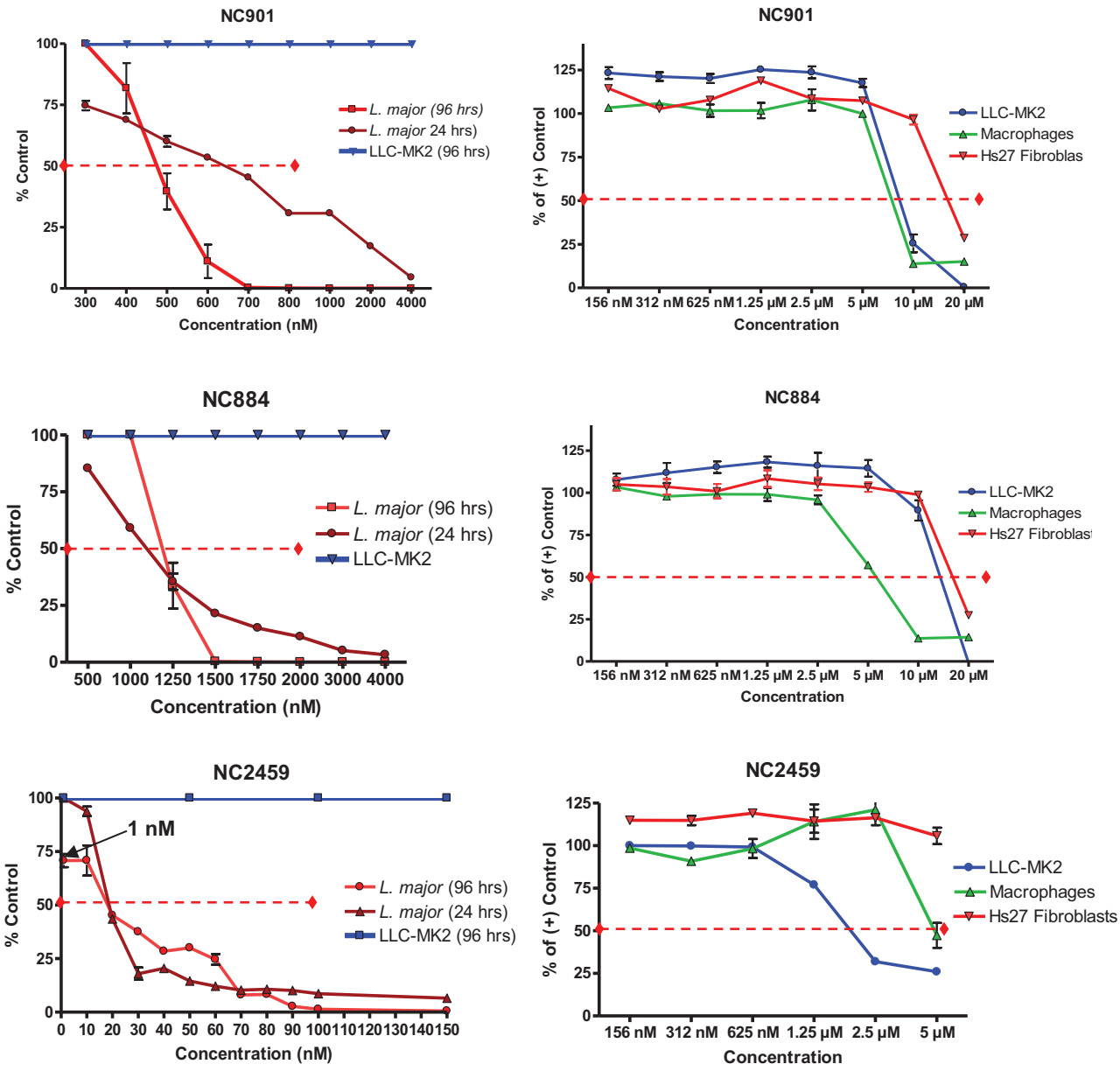

Figure 2.2: Evaluation of six candidate compounds in *L. major* and mammalian cells. On the left, the survival percentage of the parasites was determined after 24 hour and 96 hour incubation periods with compounds NC901, NC884, and NC2459. On the right, the survival percentage of the three mammalian cell lines were determined after a 96 hour incubation period with compounds NC901, NC884, and NC2459. All three compounds exhibited a much higher degree of toxicity towards the parasites than to all three mammalian cell lines. The EC_{50} was determined for each of these cell lines and is displayed on Table 2.1.

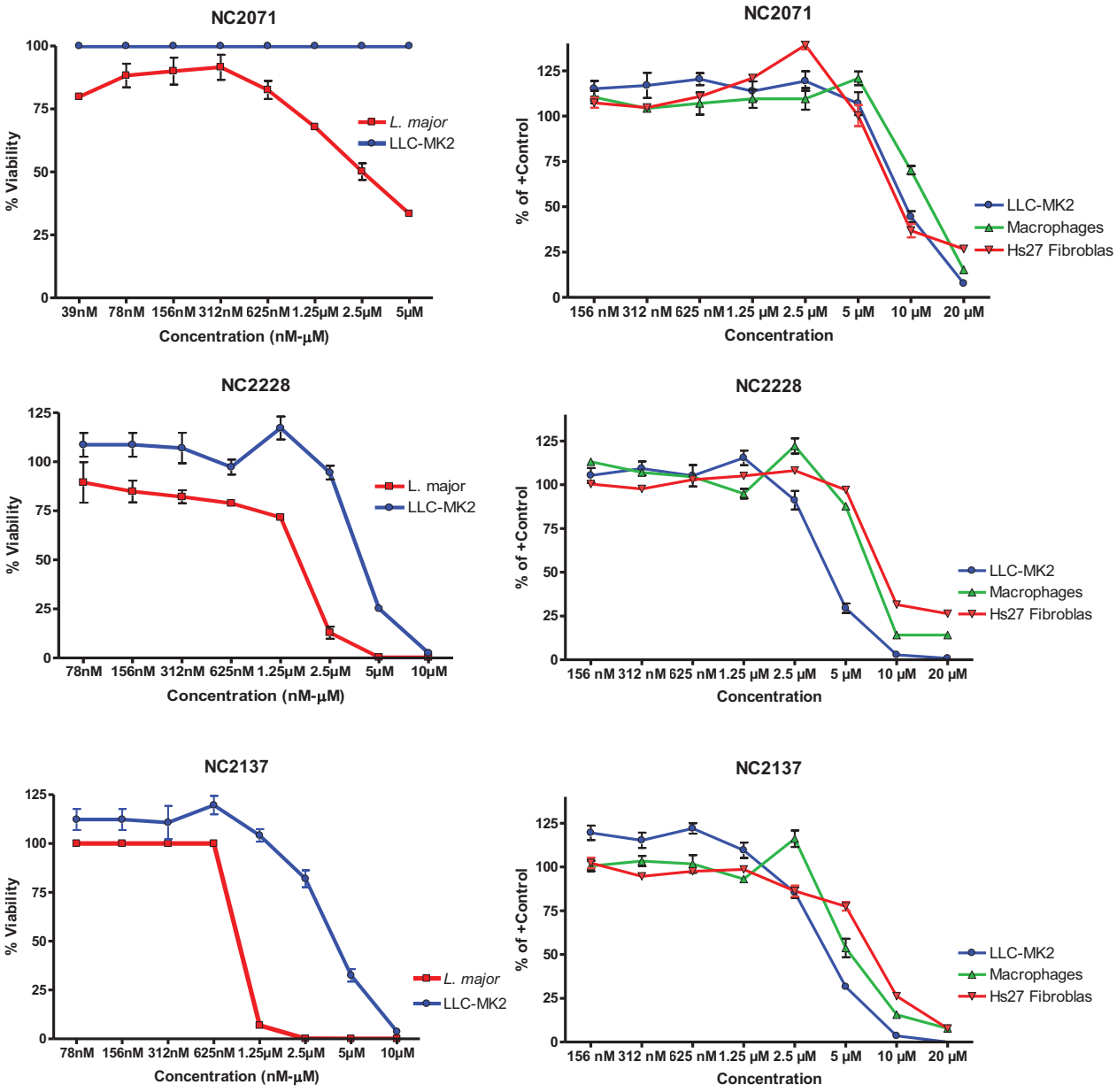

Figure 2.2 (continued): Evaluation of six candidate compounds in *L. major* and mammalian cells. On the left, the survival percentage of the parasites was determined after 24 hour and 96 hour incubation periods with compounds NC901, NC884, and NC2459. On the right, the survival percentage of the three mammalian cell lines were determined after a 96 hour incubation period with compounds NC901, NC884, and NC2459. All three compounds exhibited a much higher degree of toxicity towards the parasites than to all three mammalian cell lines. The EC_{50} was determined for each of these cell lines and is displayed on Table 2.1.

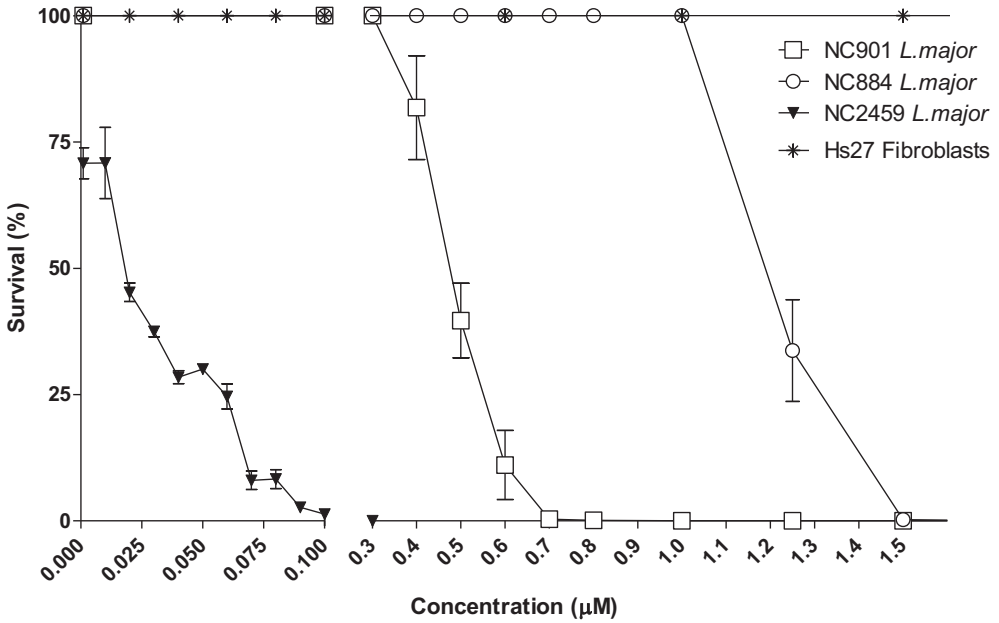

Figure 2.3: Evaluation of the leishmanicidal activity of NC884, NC901 and NC2459. The survival of the parasites and human fibroblast was determined after a 96 hour incubation period. All three compounds exhibited a much higher degree of toxicity to the parasites than to the human cell line. The EC_{50} was determined for each of these cell lines and is displayed on Table 1. (p-value < 0.0001)

To determine whether these compounds are active against *T. cruzi,* we tested the compounds (NC901, NC884, and NC2459) with non-infective epimastigote forms of *T. cruzi* from the CL Brenner and Y strains. After a 96 hour incubation period, all three compounds effectively inhibited the viability of the CL Brenner and Y strain of *T. cruzi* epimastigotes (Figure 2.4). The respective EC_{50} concentrations were 468 nM, 475 nM, and 20 nM. Therefore, not only do these compounds display toxicity towards *T. cruzi* epimastigotes, they also exhibit very similar EC_{50} concentrations required for inhibiting *T. cruzi* (Y strain) epimastigote's survival as in *L. major* promastigotes *in vitro* (Table 2.1). However, it was observed that compound NC884 had a greater than 2-fold difference in toxicity against *T. cruzi* (Y strain) as in *L. major*.

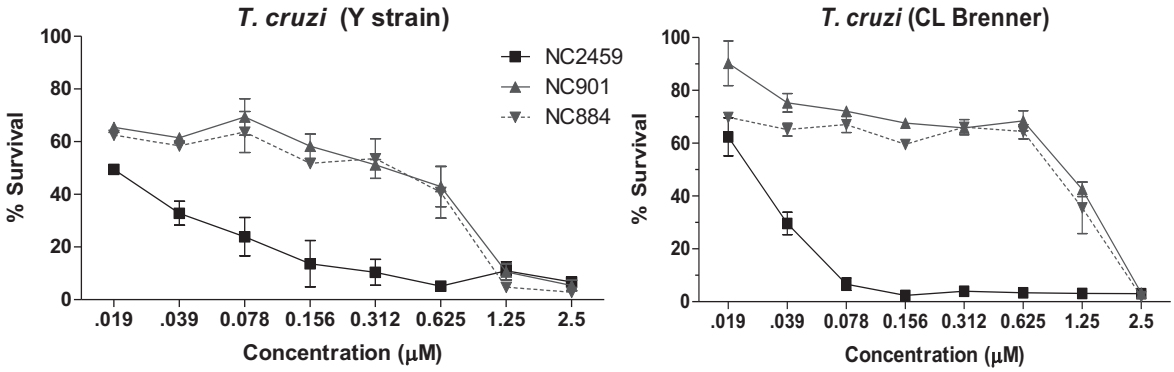

Figure 2.4: Evaluation of compounds NC2459, NC901, and NC884 in *T. cruzi* epimastigotes. The survival percentage of *T. cruzi* epimastigotes (Y strain and CL Brenner) was determined at various concentrations compound. All three compounds exhibited an EC_{50} at nanomolar concentrations as displayed on Table 1. (p-value < 0.0001)

Since Leishmania species survive and replicate within the human host as amastigotes, we wanted to determine whether these compounds have an effect on the amastigote form of the parasite. Although *L. major* cannot be cultured as amastigotes, a close relative known as *Leishmania donovani* can be induced to differentiate into amastigotes *in vitro*. At Dr. Stephen M. Beverley's lab in Washington University, *L. donovani* axenic amastigotes were treated with compounds NC901 and NC884 and showed an approximate EC_{50} of 1.25 μM and 7 μM respectively after a 96 hour treatment (Figure 2.5). This not only confirms that these compounds can have a toxic effect on the amastigote form of leishmania, but it confirms the ability for these compounds to be active against multiple trypanosomatid species. Future studies will be performed to test the effect of compound NC2459 against *L. donovani* amastigotes.

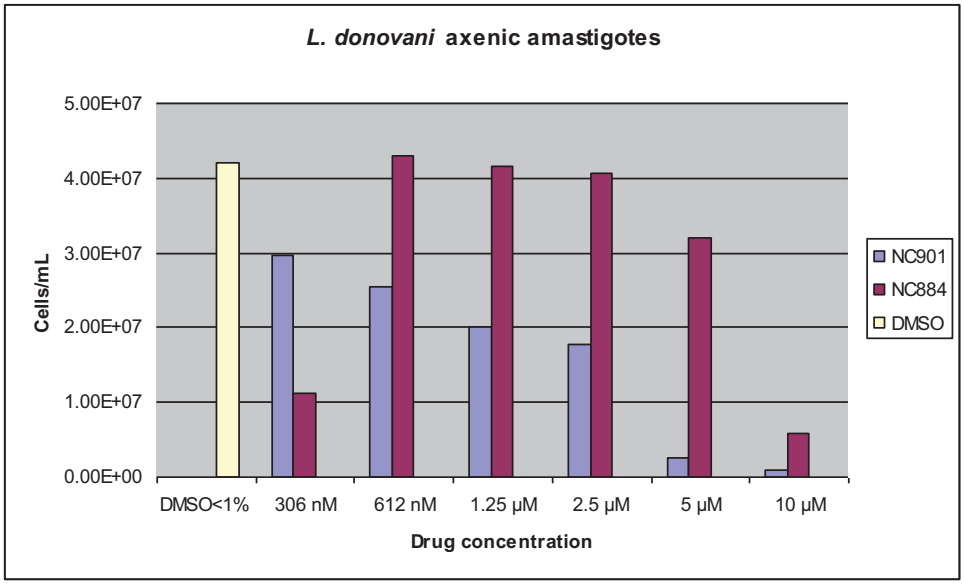

Figure 2.5: Evaluation of compounds NC901 and NC884 in *L. donovani* axenic amastigotes. These experiments were performed in 5 mL culture flasks and were incubated for 96 hours in the presence of each compound and parasites were quantified in the Beckman Coulter cell counter. *L. major* cannot be grown in culture as axenic amastigotes; therefore, *L. donovani* axenic amastigotes were tested *in vitro* against compounds NC901 and NC884. NC901 and NC884 displayed a marked decreased in the number of cells per mL after a 96 hour incubation period at 5 µM and 10 µM respectively in comparison to the negative control (1% DMSO).

Table 2.1: Summary of IC_{50} and EC_{50} for each compound (NC901, NC884, and NC2459) tested against parasites and mammalian cells. EC_{50}: Half maximal effective concentration calculated with 95% confidence interval; ± values are the estimated EC_{50} interval. TI: Therapeutic Index (IC_{50} in Hs27 human fibroblasts) / (EC_{50} in parasites). p-value < 0.0001 for all concentrations.

	Mammalian cells IC_{50} (µM) ± SD			*L. major*		*T. cruzi*	
Compounds	**Peritoneal Murine Macrophages**	**LLC-MK$_2$**	**Hs27 Fibroblasts**	**Promastigotes EC_{50} (µM) [TI]**	**Intracellular Amastigotes IC_{50} (µM)**	**Epimastigotes EC_{50} (µM) [TI]**	**Intracellular Amastigotes IC_{50} (µM)**
NC901	**7.03 ± 0.42**	**8.02 ± 0.25**	**16.0 ± 0.12**	**0.45 [35]**	**1.87 ± 0.20**	**0.468 [34.19]**	**0.301 ± 0.09**
NC884	**7.67 ± 0.31**	**15.1 ± 0.33**	**16.3 ± 0.17**	**1.12 [14.2]**	**0.937 ± 0.13**	**0.475 [33.7]**	**0.987 ± 0.11**
NC2459	**5.45 ± 0.36**	**2.0 ± 0.093**	**10.01 ± 0.09**	**0.020 [500]**	**0.625 ± 0.11**	**0.020 [500]**	**0.227 ± 0.04**

In summary, these compounds have shown to be significantly more toxic to the parasites in comparison to the mammalian cell lines (Table 2.1). Compounds NC901, NC884, and

NC2459 have shown to possess anti-parasitic effects against the insect form of both *L. major* and *T. cruzi* as well as the human form of *L. donovani*. The difference in toxicity observed between the parasites and mammalian cells led us to further experiments on intracellular amastigotes; the proliferative form of the parasites that replicate within the human host.

2.3.2 Evaluation of the anti-proliferative activity on intracellular amastigotes from *L. major* and *T. cruzi* using high-content imaging

In vitro infectivity experiments were carried out to determine the activity of compounds NC901, NC884, and NC2459 against *L. major* intracellular amastigotes. ~~Intra~~peritoneal macrophages isolated from BALB/c mice were infected with *L. major* metacyclic promastigotes. After the parasites were allowed to establish infection for 48 hours, the compounds were added and incubated for an additional 48 hours. The compounds anti-leishmanial activity was evaluated using the BD Pathway Bioimager™. In the analysis several constraints were used, such as 2, 5, and 8 or more amastigotes per macrophage. In comparison to the 1% DMSO treated control all three compounds showed a significant decrease in the percentage of infected cells under all three constraints using the unpaired *t*-test statistical analysis (Figure 2.6). The most effective concentration for compounds NC901 and NC884 was 5 μM, while compound NC2459 was most effective at a concentration of 1.25 μM. Compounds NC901 and NC884 were not as effective as the positive control amphotericin B at the same concentration of 5 μM, however, compound NC2459 was significantly more effective at decreasing the percentage of infected macrophages under the constraint of two or more parasites per macrophage.

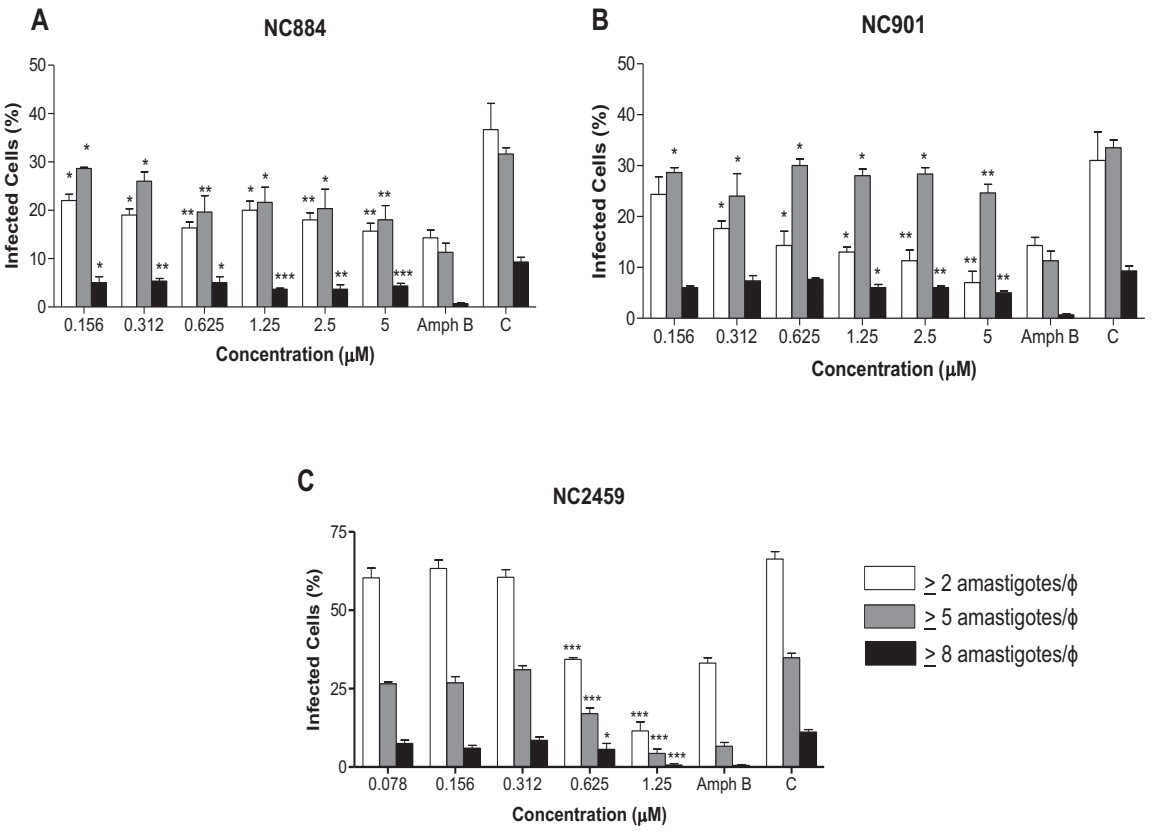

Figure 2.6: Antiproliferative activity of NC884, NC901, NC2459 on *L. major* amastigote-infected macrophages *in vitro.* Peritoneal murine macrophages were isolated from BALB/c mice and infected with *L. major* metacyclic promastigotes. 48 hours after infecting with parasites, compounds were added and incubated for 48 hours before being fixed with 4% paraformaldehyde and stained with DRAQ5®. Infected cells were analyzed using the BD Pathway™ Bioimager and screened for constraints of 2, 5, and 8 or more amastigotes per cell A). Compound NC884 given at concentrations ranging from 0.156 - 5 μM . B) Compound NC901 given at concentrations ranging from 0.156 - 5 μM. C) Compound NC2459 given at concentrations ranging from 0.078 - 1.25 μM. $p \leq 0.05$(*), $p \leq 0.01$(**), and $p \leq 0.001$(***). Amph B, Treated with 5 μM amphotericin B; C, 1% DMSO. The Z-factors calculated for the assays are in the range of 0.5 to 0.91, indicating that the quality of the assay is excellent.

Human osteoblasts were infected with *T. cruzi* trypomastigotes and were treated with each compound at multiple concentrations for 48 hours. 96 well plates were evaluated using the BD Pathway Bioimager™ and analyzed under the constraint of one or three or more amastigotes per cell (Z-factor = 0.5 indicating that is an acceptable assay). All three compounds displayed a significant decrease in the percentage of infected cells ($p \leq 0.05$ unpaired *t*-test statistical analysis)

(Figure 6). The compounds were effective in a concentration range of 156 nM to 5 µM, with the most potent compound being NC2459 exhibiting an IC_{50} of 227 nM. All three compounds were shown to be more effective than the positive control and standard drug benznidazole at 800 µM.

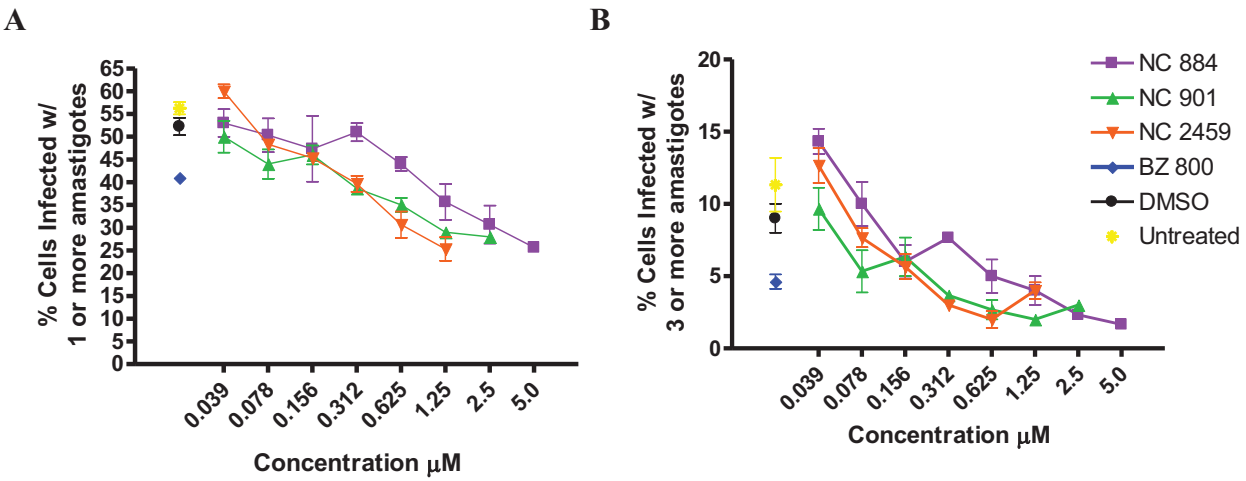

Figure 2.7: Antiproliferative activity of NC884, NC901, NC2459 on *T. cruzi* amastigote-infected human osteoblasts *in vitro.* Human osteoblasts were plated and infected with *T. cruzi* trypomastigotes. After infecting with parasites compounds were added and incubated for 48 hours before being fixed with 4% paraformaldehyde and stained with DRAQ5®. Infected cells were analyzed using the BD Pathway™ Bioimager and screened for constraints of A) 1 and B) 3 or more amastigotes per cell. $p \leq 0.05$(*), $p \leq 0.01$(**), and $p \leq 0.001$(***). BZ, 800 µM benznidazole (positive control); 1% DMSO, diluent control. The Z-factor of 0.5 indicates that the quality of the assay is good.

2.3.3 Assessment of the compounds' anti-parasitic activity on a murine model for cutaneous leishmaniasis

Two experiments were performed to explore the efficacy of the three most active compounds against *L. major* infections in BALB/c mice. In the first set of experiments (Figure 2.8), the mice were infected with 10^5 *L. major* metacyclic promastigotes as indicated in Table 2.3 below. In total there were 27 female mice separated into nine groups of three. Each group, except for those treated with amphotericin B (IP only), received two routes of administration being intraperitoneal and oral gavage given at the same concentration of drug. Drugs given through the intraperitoneal cavity were diluted in either 100% DMSO or in 1:1 DMSO:PBS.

Drugs administered orally were diluted in 1:1 SMEDDS:DMSO. It was in our interest to test our compounds with the self-microemulsifying drug-delivery system (SMEDDS) since this drug diluent is known to enhance the bioavailability of drugs that display low solubility (60). In order to test for any given effects that the drug diluents may cause we had 2 groups of controls that were given 100% DMSO through IP and 1:1 SMEDDS:DMSO through oral gavage at a volume based on the highest amount given to any individual treated mouse. As shown in Figure 2.8A, all three compounds and amphotericin B resulted in reduced footpad swelling compared to the non-treated controls throughout the course of the experiment. At 46 days post-infection all experimentally treated groups exhibited a lesion size smaller than or equal to that of the positive control group treated with amphotericin B. The mice given the oral solution of drug showed to be less effective than with DMSO through the I.P. route, therefore, the use of this method was abolished for the second set of *in vivo* experiments.

Table 2.2. Treatment regimens for *in vivo* experiments. All experiments were performed following IACUC protocol. In the hyper-infectivity experiment, the NC2459 treated group of six mice was split into two groups of three after seven days of treatment. One group remained on the same treatment, *4 mg/kg/day, for seven more days (14 total days of treatment), the other group was given double the daily dosage, **8 mg/kg/day, for 10 more days (17 total days of treatment).

Compounds	**Infection**		
	10^5	**10^6**	
	Treatment (mg/kg/day)[Time= 14 days]	**Treatment (mg/kg/day)[Time= 14 days]**	
DMSO (100 µL)	-	-	
Amp B	8	8	
NC901	2	4	
NC884	4	8	
NC2459	1	4* **[3 mice /14 days]**	8** **[3 mice /days 8-17]**

Further evidence of this result was observed by determining the relative amount of luminescence emitted from the luciferase expressing parasites in the infected footpad for each mouse in the study at 46 days post-infection (Figure 2.8B). The most effective compound at controlling the swelling of the footpad was compound NC2459. Lesions for all mice in the NC2459 treated group did not start developing measurable lesions until 2 to 3 weeks after the last treatment (total of 6-7 weeks post-infection), furthermore, one out of the three mice never developed a lesion at all after monitoring for up to twelve weeks post-infection. PCR of the *L. major* MetAP1 gene showed no traces of *L. major* genomic DNA in the footpad of the mouse displaying no lesion treated with NC2459 in comparison to the PCR from one of the infected control mice (data not shown).

To determine the relative toxicity of a compound, weights were analyzed since a reduction in weight is a good indication for toxicity of a drug (Figure 2.8C, 2.9C). There was a slight reduction in weight for all groups in the third week post-infection with a much more dramatic loss in weight for only the amphotericin B treated group. This was expected since amphotericin B is known to be highly toxic in mammalians. Mice treated with our three compounds continued to lose a slight amount of weight in the 4th week post-infection as did the DMSO treated control. This pattern of weight loss may be attributed to the physical stress (DMSO IP injections and physical manipulation) that these mice endure on a daily basis during treatment. Nevertheless, there was no significant weight loss for any of the groups except for the mice receiving amphotericin B. After treatment was abolished weights for all groups went back to normal. Additionally, no mice died as a result of the compounds toxicity.

In the *in vivo* experiment shown in Figure 2.9 (hyper-infection), mice were infected with 10^6 *L. major* metacyclic promastigotes rather than 10^5 in order to determine the activity of these

compounds in a more pronounced infection. This experiment consisted of 26 female BALB/c mice organized in four groups of five and one group of six. All experimental groups were given higher doses of compound as summarized in Table 2.2. After two weeks post-infection, prior to the first treatment, all mice displayed visible and measurable lesions five times larger than in the first trial of experiments. As shown in Figure 7B, these lesions also grew much more rapidly throughout the course of the infection than beforehand. After four weeks post-infection all three NC compounds displayed the ability to significantly reduce the lesion size in *L. major* infected mice in comparison to the control group ($p \leq 0.05$). The luminescence detected from the infected footpads for each group concurred with this observation when analyzed at 29 days post-infection (Figure 2.9B). At this time point, the mice in the control group were no longer allowed to continue the experiment to avoid physical distress caused by such a large lesion, however, all other groups were monitored for an additional four days. After one week of treatment with compound NC2459, three of the mice from this group were given double the daily dose of drug (8 mg/kg/day) while the other three remained on the same daily dose (4 mg/kg/day). The three mice given the higher dose were also treated for an extra four days of treatment or four additional daily doses. This group is referred to as NC2459 (extended treatment) as shown in Figure 2.9A. Not only did doubling the dose to 8 mg/kg/day decrease the growth rate of the lesion, but at 33 days post-infection this group had a significantly smaller lesion than all other groups ($p \leq 0.05$). The increase in dosage for the NC2459 extended treatment group did not result in any additional weight loss or toxic side effects compared to the control group, as was the case for all other treated groups (Figure 2.9C). For all groups, the removal of treatment resulted in an increase in the rate at which the lesion grew, thus the presence of compound was critical to keeping the lesion size at a minimum in this experiment.

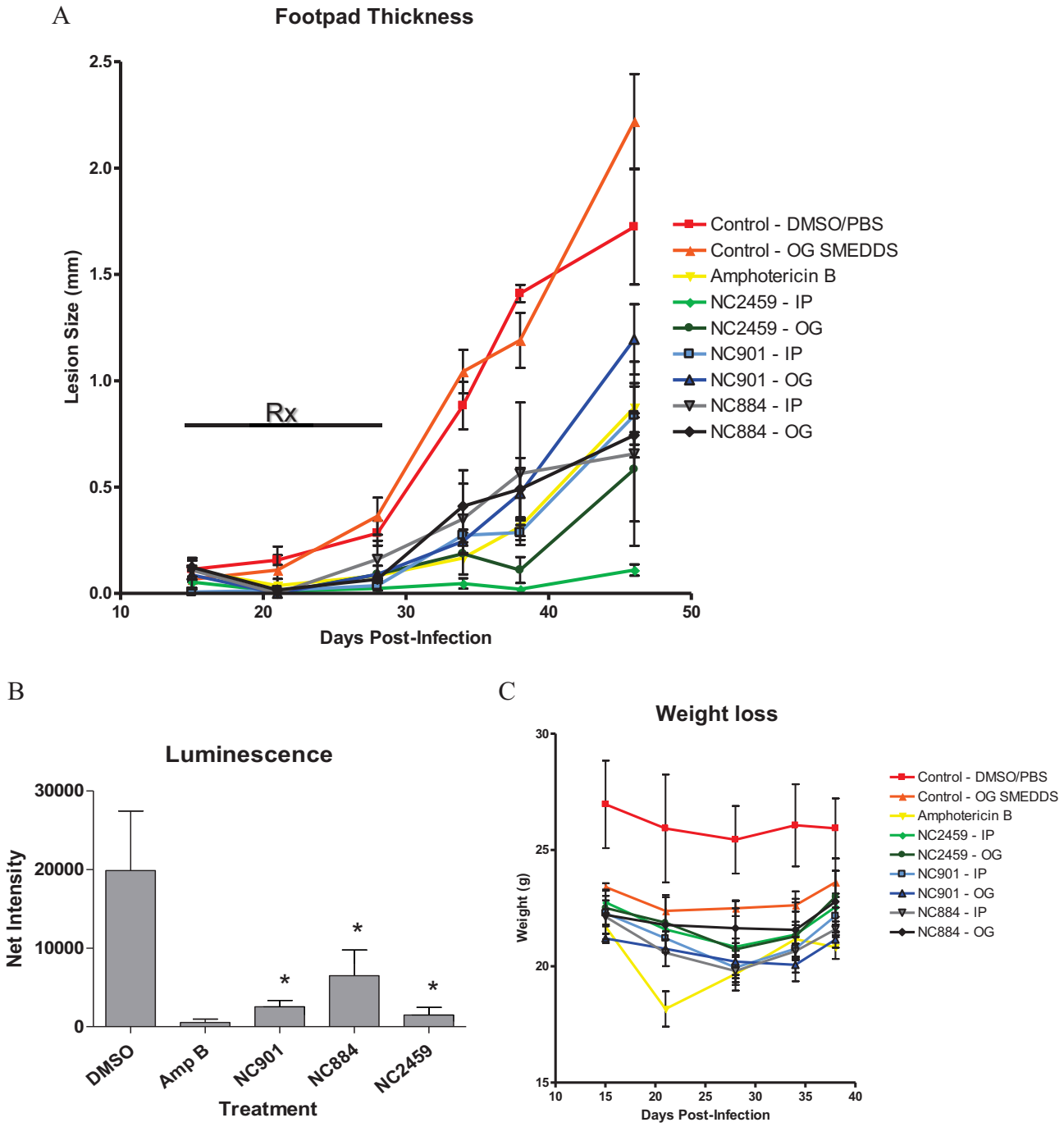

Figure 2.8: *In vivo* activity of compounds NC901, NC884, and NC2459 in BALB/c mice infected with *L. major* A) Footpad size of BALB/c mice infected with 10^5 *L. major* metacyclic promastigotes. All three compounds caused a decrease in lesion size compared to the DMSO control at 46 days post-infection. Rx line refers to the time period in which treatment was administered daily. B) Luminescence of BALB/c mice footpad at 46 days post infection. C) Weights of mice recorded throughout the duration of the experiment. Each compound resulted

in a significant decrease in lesion size in comparison to the DMSO control at 29 days p.i. ($p \leq 0.05$) Statistical analysis was carried out using the two-sided unpaired *t*-test.

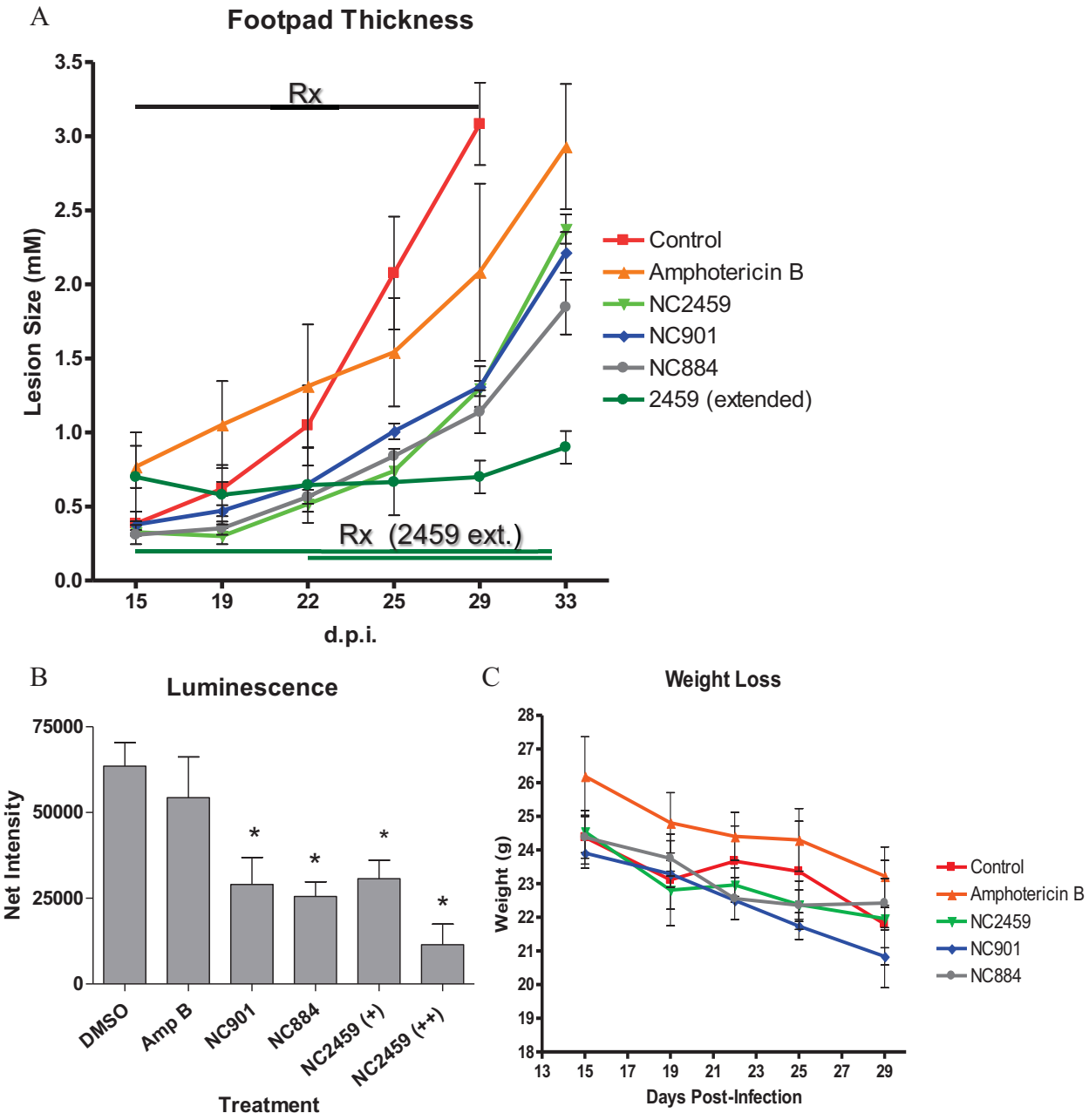

Figure 2.9. *In vivo* activity of compounds NC901, NC884, and NC2459 in BALB/c mice infected with *L. major*. A) Footpad size of BALB/c mice infected with 10^6 *L. major* metacyclic promastigotes. All three compounds caused a decrease in lesion size compared to the DMSO control at 29 days post-infection. Rx line refers to the time period in which treatment was administered daily. Double Rx line indicates that the daily dosage of NC2459 was doubled for that time period. B) Luminescence of BALB/c mice footpad determined at 33 days p.i. C)

Weights of mice recorded throughout the duration of the experiment. Each compound resulted in a significant decrease in lesion size in comparison to the DMSO control at 29 days p.i. ($p \leq 0.05$) Statistical analysis was carried out using the two-sided unpaired *t*-test.

2.3.4 α,β-Unsaturated ketones derivatives induce apoptosis-like effect and mitochondrial hyperpolarization in *L. major* promastigotes

It has been reported that some α,β-unsaturated ketones markedly increased the percentage of apoptotic cells in human pancreatic cancer cells through the depletion of intracellular thiols such as glutathione (49). Therefore, it is important to determine whether these compounds may have a similar effect on *L. major*. To assess the mode of cell death induced by candidate compounds, annexin-V/propidium iodide staining was performed. Externalization of phosphatidylserine (PS) seems to be the general feature of early stage apoptosis in most organisms, however, it has been recently reported that *L. major* promastigotes lack PS, however, upon permeabilization or miltefosine treatment annexin V binds to the parasite membrane (50). Generally, PS is the major phospholipid detected in most apoptosis assays, however, not only PS is affected during this process as during apoptosis the asymmetric lipid arrangement in the plasma membrane is compromised, resulting in extreme changes in the phospholipid composition of both leaflets (50). It was found that despite lacking PS, annexin V is able to bind other phospholipid species such as PI and PE in *L. major* promastigotes likely as a consequence of changes in the plasma membrane lipid arrangement (50). Annexin V, which has strong Ca^{2+}-dependent affinity for PS (53), was used to measure the percentage of annexin positive *L. major* parasites and macrophages in response to treatment with compounds NC901, NC884, and NC2459. The annexin V^-/PI^- population was regarded as normal cells, while positive staining just for annexin V was used as a measure of early changes in the lipid arrangement of the plasma membrane and annexin V^-/PI^+ was related to late changes in the lipid

arrangement of the plasma membrane or necrosis. As shown in Figure 2.10A, it was observed that all three compounds significantly induced an apoptosis-like effect in *L. major* promastigotes in comparison to the 1% DMSO treated controls. In order to determine whether these concentrations of drug that have shown to be toxic to the parasites are inducing apoptosis in mammalian cells, we tested the same concentrations in isolated intraperitoneal macrophages from BALB/c mice. As shown in Figure 2.10B, no effect was observed in the macrophages treated with our three candidate compounds at the same concentrations that induced a significant percentage of annexin positive cells in *L. major* promastigotes.

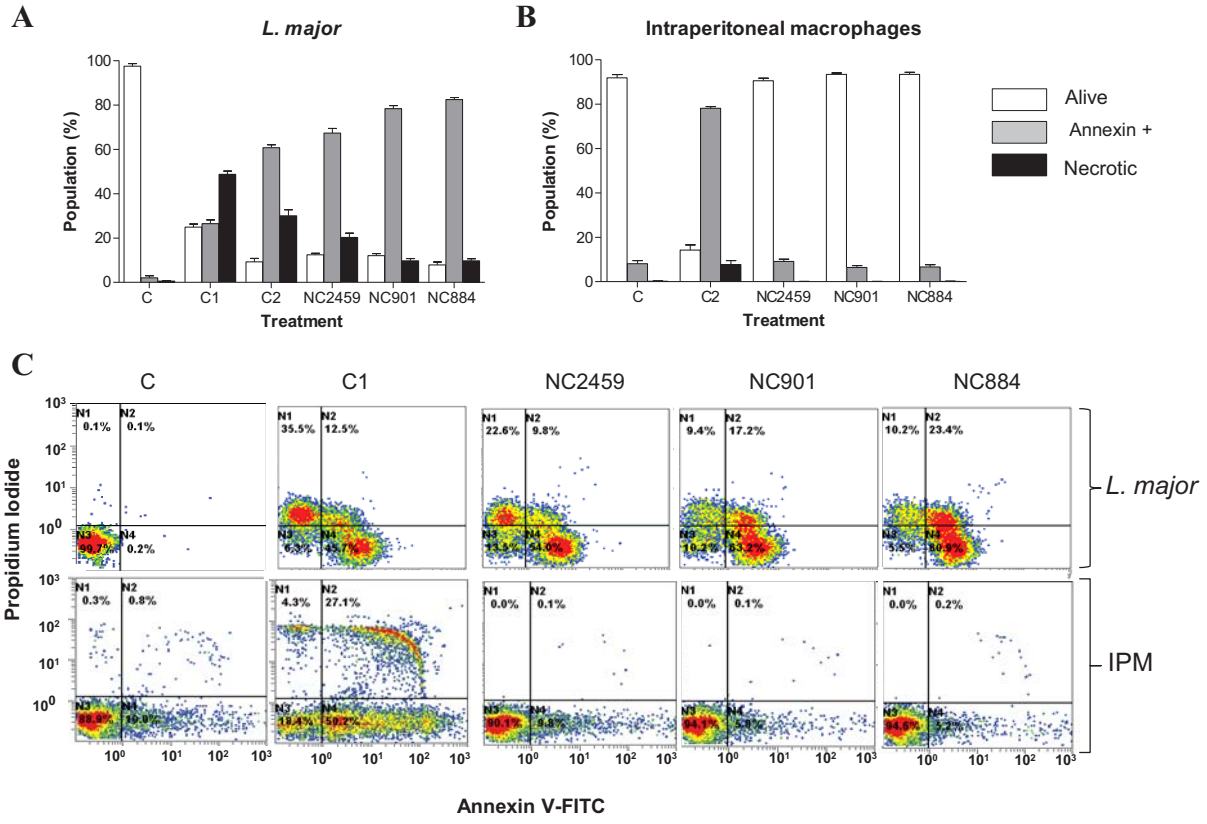

Figure 2.10. The compounds NC901 (2.5 µM), NC884 (2.5 µM), and NC2459 (312 nM) induce annexin binding in *L. major* promastigotes and not in murine intraperitoneal macrophages at concentrations that are toxic to parasites. A-B) Percentages of parasites and macrophages emitting green fluorescence signal (annexin +) or red fluorescence signal (necrotic). C) Representative flow cytometric dot plots used to quantify the percentages of green and red signal. IPM, BALB/c mice isolated intraperitoneal macrophages. *L. major* promastigotes and IPM treated were analyzed using Annexin-V/propidium iodide staining. C, negative control cells

treated with 1% DMSO; C1, necrosis control parasites treated with 2 mM H_2O_2; C2, apoptosis control cells treated with 200 μM H_2O_2 in *L. major* and 2 mM H_2O_2 in macrophages.

The disruption of the mitochondrial membrane potential ($\Delta\psi_m$) is a characteristic feature of apoptosis (48) and other forms of cellular disfunction and death. Both in multicellular and unicellular organisms, the mitochondrion is an important cellular source for the generation of reactive oxygen species (ROS) inside cells, which serve as inducing signals for apoptosis (54). To determine the changes in the $\Delta\psi_m$ we used the Mitoprobe™ JC-1 assay. JC-1 exhibits potential dependent accumulation in mitochondria, indicated by a fluorescence emission shift from green (~529 nm) to red (~590 nm). A mitochondrial membrane potential disrupter known as CCCP (carbonyl cyanide 3-chlorophenylhydrazone) was used as our positive control. As shown in Figure 2.11, all three candidate compounds caused a concentration dependent loss in $\Delta\psi_m$ in comparison to the negative control treated with 1% DMSO. Therefore, our results suggest that the apoptosis-like effect induced by compounds NC901, NC884, and NC2459 in *L. major* promastigotes is mitochondrial dependent.

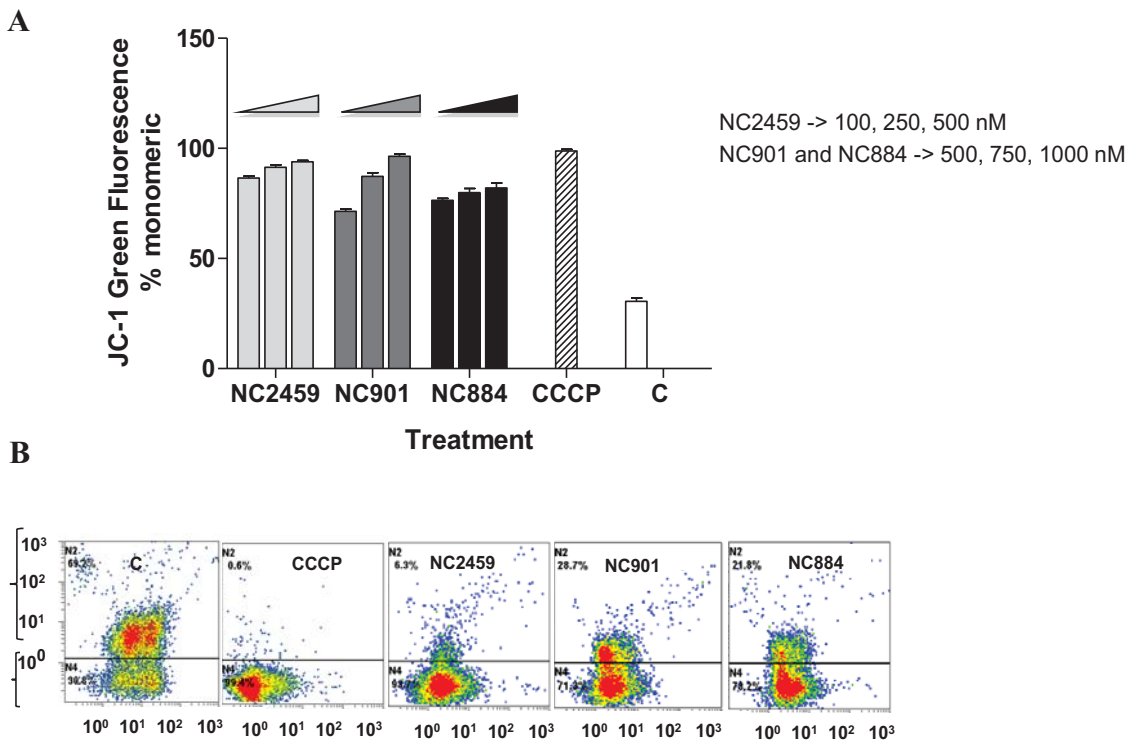

Figure 2.11: Mitochondrial membrane depolarization of L. major promastigotes treated with the enone compounds NC884, NC901 and NC2459. The parasites were treated with several concentrations of the NC compounds and analyzed using the Mitoprobe™ JC-1 assay. C, negative control 1% DMSO; CCCP (50 µM), positive control. A) Percentages of parasites emitting green fluorescence in response to treatment. B) Representative flow cytometric dot plots used to quantify the percentages of green signal. Mitochondrial membrane depolarization of L. major promastigotes treated with the enone compounds NC884, NC901 and NC2459 The parasites were treated with several concentrations of the NC compounds and analyzed using the Mitoprobe™ JC-1 assay. C, negative control 1% DMSO; CCCP (50 µM), positive control. A) Percentages of parasites emitting green fluorescence in response to treatment. B) Representative flow cytometric dot plots used to quantify the percentages of green signal.

Mechanistic studies

To determine the possible mechanism of action of these compounds we analyzed the characteristics of the NC library as well as the structure of compounds NC901, NC884, and NC2459. The compound library was originally designed as antineoplastic agents that have a preferential affinity towards cellular thiols rather than hydroxy and amino functionalities present

in nucleic acids. Each compound has the ability to cause two or more successive alkylations of cellular thiols (Fig. 2.12A-B). One result of this reaction in cancer cells is a decrease in the cellular levels of glutathione. Also, some of these compounds are known to inhibit the isozyme of glutathione-*S*-transferase (33). These facts provoked the question, "What essential molecules or enzymes within the parasites can be affected by the alkylation of thiols?" Consequently, we decided that these compounds may be interacting with the major trypanosomatid pathway involved in thiol metabolism. This essential pathway known as trypanothione metabolism is unique to trypanosomatids and includes the enzyme trypanothione reductase (TR). TR is in charge of keeping trypanothione in the reduced, di-thiol state allowing the molecule to carry out many essential functions. Also, trypanothione is synthesized through the conjugation one molecule of glutathione to one molecule of spermidine. This may foreshadow the possibility that this molecule is being subject to alkylation when presented with these compounds as the case is for glutathione in cancer cells (33). Moreover, lipoamide dehydrogenase (LADH) is an enzyme that is both structurally and mechanistically related to TR and may be responsible for the role of the TR/trypanothione redox system within mitochondria of trypanosomes (27). The substrate of LADH, dihydrolipoamide, relies on the presence of a single thiol group to carry out many of its functions as well making it a possible target that is susceptible to alkylation by these compounds (27). These characteristics of the compound library led to the speculation that TR and LADH may be the target enzymes for these three compounds.

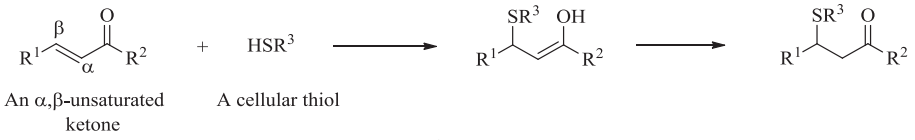

A

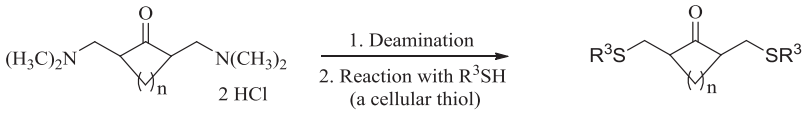

NC 901: n=2
NC 884: n=3

B

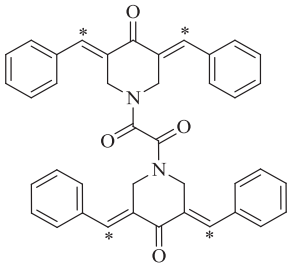

NC 2459

* Site of attack of cellular thiols

C

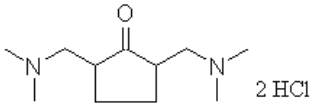

NC 901

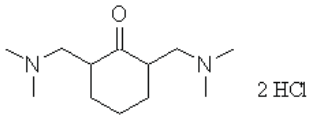

NC 884

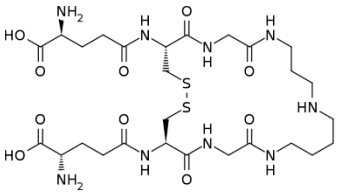

Trypanothione

D

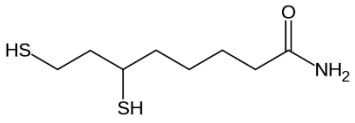

Dihydrolipoamide

Figure 2.12: A. The reactions of α,β-unsaturated ketones with thiols. B. Structures of NC901 and NC884 as well as the perceived manner in which reaction with thiols takes place. C. Structure of NC2459 indicating the potential sites where interactions with thiols can occur. D. Structures of NC901, NC884, trypanothione (ox) and dihydrolipoamide.

In collaboration with Dr. Luise Krauth-Siegel, they were able to test the ability of compounds NC901 and NC884 to inhibit the enzymatic activity of the recombinant proteins TR and LADH from *T. cruzi* at the University of Heidelberg in Heidelberg, Germany. When tested against these enzymes, both compounds displayed a time dependent irreversible inhibition (Figure 2.13). For the TR enzymatic assay, compound NC901 caused a dramatic decrease in enzymatic activity with 100% inhibition after 90 minutes at 100 μM. Compound NC884 was not as effective at inhibiting TR with only 54% inhibition after 180 minutes at 100 μM.

As for LADH, these compounds had a much more pronounced effect on the activity of this enzyme. LADH was inhibited by 81% after being incubated with compound NC884 for 120 minutes at 100 μM. Again, NC901 was more effective at inhibiting this enzyme causing nearly complete inhibition after only 15 minutes at 100 μM and an 89% inhibition after 30 minutes at 50 μM. These results indicate that TR and LADH may be affected by compounds NC901 and NC884. The high concentrations used to inhibit these enzymes may suggest that they are not the primary targets of these compounds. Lower concentrations of drug need to be tested before making any further conclusions.

A

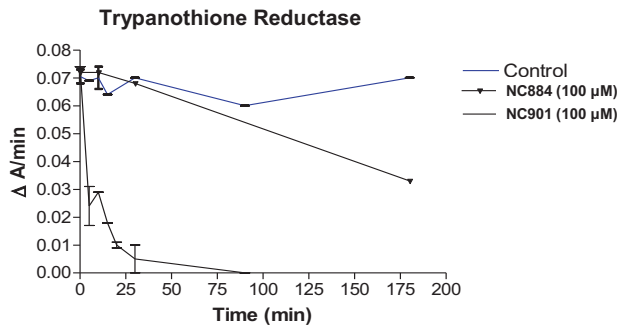

Time (min)	NC884 (100 μM) Inhibition (%)	NC901 (100 μM) Inhibition (%)
15		76
30	5	93
90		100
180	54	

B

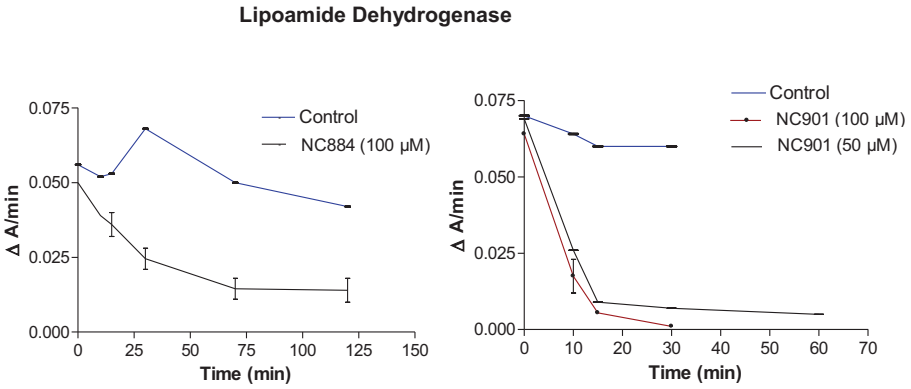

NC884 (100 µM)

Time (min)	Inhibition (%)
0	
10	34
15	42
30	60
60	74
120	81

NC901 (100 µM)

Time (min)	Inhibition (%)
0	
5	64
10	92
15	98

NC901 (50 µM)

Time (min)	Inhibition (%)
0	
5	62
15	87
30	89
240	92

Figure 2.13: Enzymatic activities of TR and LADH in response to NC901 and NC884. Trypanothione reductase (A) and lipoamide dehydrogenase (B) enzymatic assays for compounds NC901 and NC884. Data is expressed as a change in enzymatic activity per minute. Compounds NC901 and NC884 showed a time dependent inhibition of TR (A) and LADH (B). Inhibition was determined to be irreversible. Enzymatic assays were performed by Krauth-Siegel *et al* at the University of Heidelburg.

2.4 Discussion

In the discovery of novel anti-parasitic drugs, the similarities between cancer cells and eukaryotic parasites have become intriguing to many scientists and many are thus exploring the idea of using anti-cancer drugs in anti-parasitic therapy (55).

Following this idea, α,β-unsaturated ketone derivatives (NC series), initially developed as anti-cancer drugs, were evaluated against *L. major* promastigotes, *T. cruzi* epimastigotes and four types of mammalian cells. The majority of the 136 compounds screened using our HTS assays displayed a high degree of cytotoxicity towards *L. major* promastigotes with a low degree of toxicity towards the LLC-MK_2 cells (Figure 2.1). Upon further evaluation of the difference in

toxicities between the parasites and different mammalian cell types, three (NC901, NC884, and NC2459) of the 136 compounds in the drug library showed potent anti-parasitic activity with no cytoxicity to the mammalian cells tested at low nanomolar-micromolar concentrations that were very active against *L. major* promastigotes (Figure 2.2). These exciting findings led us to determine whether or not these three compounds are active against a related pathogenic trypanosome, *T. cruzi*. Analysis of these three compounds on the insect form of *T. cruzi* resulted in similar EC_{50} values observed in *L. major* promastigotes (Figure 2.4). The most potent compound, NC2459, had a minimum of a 100-fold difference in toxicity between both parasites and all mammalian cell types tested.

The activity of these three compounds was analyzed against the intracellular forms of *L. major* and *T. cruzi* in infectivity assays. These experiments are important in determining the potential activity of a given compound *in vivo* since we are treating the parasites while replicating within their natural host cells. It was observed that all three compounds (NC901, NC884, and NC2459) significantly reduced the parasite burden in *L. major* and *T. cruzi* infected mammalian cells (Figures 2.6 and 2.7, respectively).

Next, the importance of these findings was confirmed by performing an analysis of the three compounds in an *in vivo* model for cutaneous leishmaniasis. Our findings demonstrated the ability of these compounds to reduce the physical burden caused by these parasites within a localized area without any obvious toxic side effects when treated through the intraperitoneal route. In Figure 2.8, compounds NC901 and NC884 reduced the footpad swelling similar to that of the positive control (Amph B), while compound NC2459 clearly exhibited a much lower amount of swelling than all groups. In the second treatment (Figure 2.9), the dosages were increased and all experimental groups showed significantly smaller lesion sizes than that of the

control group at four weeks post-infection, while compound NC2459 given at 8 mg/kg/day was much more effective than all treated groups at 33 days post-infection. There were also no signs of toxicity in all experimentally treated groups in the hyper-infection experiment.

It has been previously reported that various enones or thiol alkylators such as the compounds tested in this study have shown to induce apoptosis in pancreatic cancer cells through the depletion of mitochondrial glutathione (GSH) (49). Therefore, to further understand the mechanism of action in the parasite it was determined that compounds NC901, NC884, and NC2459 induce annexin V binding in *L. major* promastigotes at concentrations that do not affect intraperitoneal macrophages (Figure 2.10). Moreover, our results strongly suggest that the induction of this apoptosis-like effect in *L. major* promastigotes is mitochondrial dependent as treatment of these parasites with all three compounds resulted in the depolarization of the mitochondrial membrane potential ($\Delta\psi_m$) (Figure 2.11). These findings are important in deciphering the mechanism of action of these compounds and determining whether or not these compounds have a similar mechanism as reported in pancreatic cancer cells.

Based on the characteristics of the NC library, we suggest that these compounds may be interfering with the essential trypanosomatid unique pathway known as thiol or trypanothione metabolism. Some of these previously established characteristics include the ability for these compounds to target cellular thiols and lower cellular levels of glutathione as well as inhibit the isoenzyme of glutathione *S*-transferase in human pancreatic cell lines (49). Additionally, these compounds are known to be cytotoxic thiol alkylators, meaning that they have the capability to spontaneously react with thiol groups present in low molecular weight molecules (49). Preliminary unpublished data from our lab in collaboration with Dr. Krauth-Siegel *et al*. has shown that compounds NC901 and NC884 are irreversible inhibitors of the primary enzyme

involved in the trypanothione pathway, trypanothione reductase (TR) from *T. cruzi*, as well as a structurally and functionally similar enzyme, known as lipoamide dehydrogenase (LipDH) also from *T. cruzi*. These two enzymes both play many critical roles within all stages of the parasites' life cycle including the responsibility of eliminating toxic ROS that is constantly encountered by the parasite as well as many other essential functions (25). Both compounds NC901 and NC884 exhibited a time-dependent irreversible inhibition of both enzymes with LipDH exhibiting a more significant level of inhibition than TR (Figure 2.13). Interestingly, the compound that was more cytotoxic towards the parasites (NC901) was also the more potent inhibitor of these two enzymes. The inhibition of LipDH needs to be further studied since it was reported that some thiol alkylators react with mitochondrial GSH in pancreatic cancer cells leading to a number of pathological effects such as accumulation of ROS, oxidation of the cellular GSH pool, and apoptosis (49). It has been suggested that LipDH has the role of activating thiol containing molecules such as trypanothione and tryparedoxins within the mitochondrion of *T. cruzi* which are in charge of countering toxic ROS that accumulates within this organelle (28). Therefore, inhibition of LipDH within the mitochondrion of *L. major* and *T. cruzi* may be causing adverse effects in the parasites as we were able to determine that the integrity of the mitochondrial membrane is being compromised by the compounds in this study. Subsequently, the inhibitory action of the lead compound NC2459 on both enzymes also would be assessed. Further tests are in progress to confirm whether or not these enzymes are the primary target of these compounds or whether the substrates of TR and LipDH, trypanothione and dihydrolipoamide respectively, are being targeted. The latter would be quite possible since these compounds are known to be thiol alkylators and the substrates trypanothione and dihydrolipoamide both require two thiol groups in order to be in their active forms (25). It has been established that these molecules

carry out many essential functions within both *L. major* and *T. cruzi* parasites (25). The fact that these compounds have very similar effects and EC_{50} values against different species of parasite may indicate that they are acting on the substrates which are structurally identical in these parasites. It is plausible that these compounds may be inhibiting TR and LipDH as well as their substrates resulting in a compounded negative effect against the parasites. This is known to be the case for the compound melarsenoxide which is currently used to combat *Trypanosoma brucei*, the causative agent of African sleeping sickness. Melarsenoxide inhibits TR and LipDH while forming stable 1:1 complexes with dithiols trypanothione ($T(SH)_2$) and dihydrolipoamide (56). This would be an exciting explanation as to why these compounds are far more toxic to the parasites than they are to the mammalian cells.

In summary, three compounds displaying significant cytotoxicity towards *L. major* promastigotes and amastigotes as well as *T. cruzi* epimastigotes and amastigotes were discovered from the NC antineoplastic drug library. All three compounds showed a very low level of toxicity towards three separate mammalian cell lines and in BALB/c mice. More importantly, our studies have shown that these compounds are capable of reducing the parasite burden of *L. major* induced cutaneous leishmaniasis *in vivo*. Based on the promising results obtained here further studies are underway to determine the precise mechanism of these compounds. These findings also provide evidence that anti-cancer drugs may serve as suitable agents for pursuing new types of compounds targeting trypanosomatids.

The data obtained in this present study suggests that enones could be useful as a safe alternative to the current clinical drugs used to treat leishmaniasis and Chagas' disease. Further studies into the mechanism of action of these compounds are still required.

Chapter 3: Evaluation of Pyruvate Phosphate Dikinase as Chemotherapeutic Target

3.1 Materials and Methods

3.1.1 Construction of PPDK/PAC

The 5’ untranslated region (5' UTR) of the *PPDKTc* gene was amplified using the oligonucleotides 5' UTR sense (5’-GCGGCCGCCTCTTTATGGAGGCCGCAATC-3’) and 5' UTR antisense (5’-ATCGATCATAATGCCTTTG TTTTTCACTTTAT-3’). Next, the 3' UTR of the PPDK*Tc* gene was amplified using 3' UTR-sense (5’-CTCGAGAAGGATTTTGAGGCATTACGGTG-3’) and 3' UTR-antisense (5’-GGGCCCAAGACGCACCCATTGTGGAAC-3’). Puromycin N-acetyltransferase (PAC) was amplified using PAC-sense (5’-ATCGATATGACC GAGTACAAGCCCACG-3’) and PAC-antisense (5’-CTCGAGTCAGGC ACCGGGCTTGCGG-3’). Polymerase chain reaction (PCR) was performed with an initial denaturation of 5 minutes at 95°C, followed by 39 cycles of 60 sec at 95 °C, 60 sec at 56 °C and 45 sec at 72 °C, a final 10-min elongation at 72 °C was performed. Each individual fragment was then cloned into pGEM-T easy (Promega) and subsequently into pBluescriptSK. 5'-UTR was digested with *NotI* and *ClaI,* 3'-UTR with *XhoI* and *ApaI* and PAC with *ClaI* and *XhoI* prior to being ligated into pBluescriptSK.

3.1.2 Transfection

Epimastigote forms of the parasite (Y strain) were washed once with electroporation buffer (137 mM NaCl, 21 mM HEPES, 5mM KCl, 5.5 mM NaHPO4, 0.77 mM glucose, pH 7.0) and resuspended in the same buffer at a density of 1 x 10^8 cells/mL. Then 200 µL of cell suspension were placed into a 0.2-cm electrode gap cuvette with 30 ng of PPDK/PAC linearized with *ApaI*. The electroporator (GenePulser II, BioRad) was set to give 3 pulses of 325 V, 500 µF. Electroporated parasites were placed in 1 mL of liver infusion tryptose (LIT) medium. After 24

hours, 2μg/mL of puromycin was added. Surviving transfectants were cloned by serial dilution in 96-well plates.

3.1.3 Sothern Blot Analysis

The PPDK*Tc* gene was amplified using primers PPDK-sense (5'-GAATTCATGGAATCCAAAAAGTTTGTTTACTAC-3') and PPDK-antisense (5'-AAGCTTCTACAGCTTGGCGGCGATCGC-3'). The fragment was then digested using *Pst*I, yielding a fragment of ~ 700 bp that was used as a probe. The plasmid pGEM/PAC mentioned above was digested using *ClaI* and *XhoI* and the resulting fragment was used as a probe to screen for PAC. The probes were then labeled with an alkaline phosphatase enzyme (Amersham, GE Healthcare). 5 μg of each genomic DNA from transfected and wild type parasites (Dm28c strain) were digested with *Pst*I. Following separation by electrophoresis in 1% agarose gel, and transfer to positively charged nylon membrane (Hybond), hybridization and signal detection were performed using the Gene Images AlkPhos Direct Labelling and Detection System (Amersham, GE Healthcare), according to manufacturer's instructions.

3.1.4 Expression of *PPDKTc*

The PPDK*Tc* gene was amplified from *T. cruzi* genomic DNA with primers PPDK-sense (5'-GAATTCATGGAATCCAAAAAGTTTGTTTACTAC-3') and PPDK-antisense (5'-AAGCTTCTACAGCTTGGCGGCGATCGC-3'), and then cloned into DH5α *E. coli* using the pGEM-T easy vector. It was then digested with *EcoR*I and *Hind*III and ligated in between these sites in the bacterial expression vector pET28a. This vector contains a kanamycin resistance

gene, which confers resistance in the host in positive clones. The resulting plasmid pET28a/PPDK was transformed into *E. coli* (BL-21) cells and grown on LB/kanamycin plates for positive colonies. One colony was picked and grown in 10 mL LB/kanamycin liquid media overnight at 37°C. The following day the 10 mL culture was added to 190 mL of LB/kanamycin. Protein expression was induced with 200 μL of 1M IPTG and 1 mL samples were taken at 0, 1, 2, 3, and 4 hours to test for the optimum time of expression. At optimum time cells were centrifuged at 4,000 rpm for 10 minutes. The pellet was lysed with B-PER (Thermo-scientific) reagent and sonicated until the pellet was completely dissolved. This was then centrifuged at 14,000 g for 20 minutes. The resulting pellet is considered to be the insoluble fraction and the supernatant is the soluble fraction.

3.1.5 Expression of *PPDKLm*

The PPDK*Lm* gene was amplified from *L. major* genomic DNA with primers PPDK*Lm*-sense (5'-GGATCCATGGACACCGTTAAGCACGT-3') and PPDK$_{Lm}$-antisense (5'-GAGCTCTTACAGCTTAGAGCCAGCCAG-3'), and then cloned into DH5α *E. coli* using the pGEM-T easy vector. It was then digested with *Bam*I and *Sac*I and ligated in between these sites into the bacterial expression vector pRSETa. This vector contains an antibiotic resistance gene, which confers resistance in the host in positive clones. The resulting plasmid pRSETa/PPDK$_{Lm}$ was transformed into BL-21 *E. coli* cells and grown on LB/ampicillin plates for positive colonies. One colony was picked and grown in 10 mL LB/ampicillin liquid media overnight at 37°C. The following day the 10 mL culture was added to 190 mL of LB/ampicillin. Protein expression was induced with 200 μL of 1M IPTG and 1 mL samples were taken at 0h, 1h, 2h,

3h, and 4h to test for the optimum time of expression. At optimum time cells were centrifuged at 4,000 rpm for 10 minutes. The pellet was lysed with B-PER (Thermo-scientific) reagent and sonicated until the pellet was completely dissolved. This was then centrifuged at 14,000 g for 20 minutes. The resulting pellet is considered to be the insoluble fraction and the supernatant is the soluble fraction. The soluble fraction was collected and $PPDK_{Lm}$ protein was purified with a HisTrap Column using Fast Protein Liquid Chromatography (FPLC) as previously described (57).

3.1.6 Generation of PPDK inhibitors' library

Generation of the PPDK inhibitors' library was performed in collaboration with Enamine. First, a virtual screening was performed among the known PPDK inhibitors described in the literature to select promising structures. Next a similarity search was used based on topological fingerprints of known compounds. Then, a docking technique was performed for the virtual screening to substantially increase chances for the discovery of PPDK inhibitors from new chemical classes. For this purpose the 3.0-Å resolution crystal structure of glycosomal pyruvate phosphate dikinase from *T. brucei* (PDB ID 2X0S) was used. Missing residues within the active site were reconstructed using simulated annealing followed by MD. To perform an accurate docking study followed by processing of resulted complexes we used a tune docking algorithm with known small molecule inhibitors. Once we receive reproducible docking results and generate plausible binding models, the reconstructed crystal structure will be screened against an Enamine compound collection of drug-like small molecules. Based on developed binding models we will process generated complexes to extract those that strictly correspond to tight binding hypothesis. At the end of the virtual screening we expect to generate a focused library with up to

2,000 compounds (~1000 from ligand based approach and ~1000 from docking study) to be screened *in vitro*. Based on our previous experience, we are confident that focused libraries of this size based on the comprehensive virtual screening are sufficient to obtain initial hit compounds. Once the initial hits are identified, a quick follow up of libraries based on chemical scaffold similarity to the hits will be designed and screened.

3.1.7 Preparation and Analysis of PPDK Inhibitors Library for Screening

The compound library containing 222 compounds was shipped in glass vials containing 1 mg of each compound. Each compound was diluted in DMSO to a final concentration of 5 mM. Each compound was transferred to 96-well drug plates at stock concentrations as well as 1:10 stock dilutions. Two microliters of each drug was automatically transferred from each well to a corresponding well in a plate containing parasites or mammalian cells using the epMotion automated pipetting system. This gives a final concentration of 50 μM when transferred from the stock plate and 5 μM when transferred from the 1:10 stock dilution plate. Viability of the *L. major* parasites and the Hs27 fibroblasts were analyzed as previously described above.

3.2 Hypothesis

Disrupting the availability or activity of PPDK will reduce the viability and infectivity of *L. major* and/or *T. cruzi* to a therapeutically effective degree.

3.3 Results

3.3.1 Knockout of *PPDKTc*

Knockout of the pyruvate phosphate dikinase gene is necessary to determine the requirements for activity of this enzyme for viability and infectivity of *T. cruzi*. However, in kinetoplastids attempts to knockout an essential gene invariably leads to the generation of an extra copy as a result of selective chromosomal polysomy (58). The knockout in this case is only possible upon simultaneous expression of the coding region of the target gene from an episome (58). Consequently, the strategy to obtain the *PPDKTc* null mutant consists of three steps (Figure 3.1): a) create the mutant pPPDKTcGFP of *T. cruzi* Y strain by cloning *PPDKTc* into the trypanosomatid expression vector pTEX-GFP; b) to knockout the PPDK in the first allele and replace it with the resistance gene puromycin acetyl-transferase (PAC) through homologous recombination; and c) to perform the knockout in the second allele and replace it with hygromycin through homologous recombination. Steps b and c will be attempted in WT as well as in the pPPDKTcGFP expressing parasites in step a.

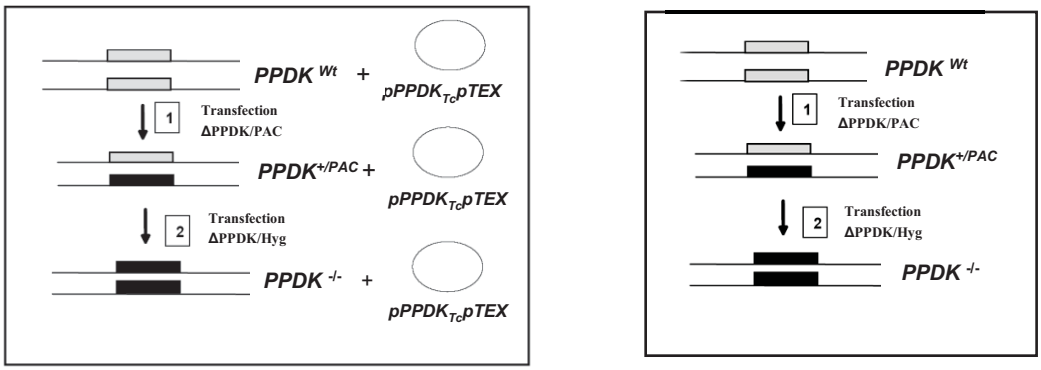

Figure 3.1: Schematic representation of the strategy to accomplish the knockout of PPDK$_{Tc}$.

First, WT *T. cruzi* (Y) parasites were transfected with the PPDK/PAC construct. The first several attempts resulted in all of the parasites dying 1-2 weeks after treatment with

puromycin at 2 µg/mL. Eventually, one of the transfectant cultures survived longer than the previous cultures in the presence of drug. Genomic DNA was purified from this culture and digested at various regions for analysis (Figure 3.2). PCR of the gDNA from the transfected cells with PAC oligonucleotides resulted in a positive band (600 bp) in only the parasites transfected with the construct (Figure 3.2). However, Southern blot analysis with the PAC probe resulted in no detection of any hybridization with gDNA from transfected parasites or with wild type DNA. To overcome this problem, we will repeat southern blot analysis using the more sensitive radioactively labeled probes.

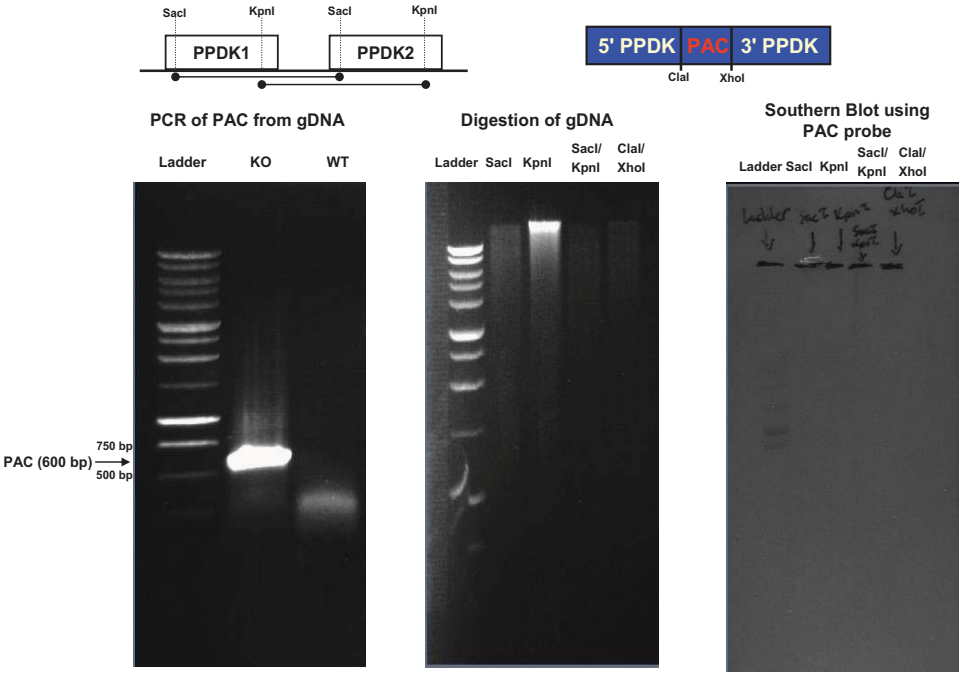

Figure 3.2: DNA gel and Southern blot of gDNA from PPDK/PAC transfected epimastigotes. PCR of transfected and WT parasites (left), digestion of gDNA ran in 1% agarose gel (middle) at specific restriction sites (above), and Southern blot analysis of *T. cruzi* cultures transfected with PPDK/PAC construct (right).

3.3.2 Expression of $PPDK_{TC}$

Expression and purification of the recombinant PPDK protein from *T. cruzi* will allow us to test the specificity of PPDK inhibitors in enzymatic assays. Also, highly purified PPDK enzyme will allow our lab to use this protein for future crystallography studies in order to better understand its structure and function. After successfully cloning $PPDK_{TC}$ into pET28a we were able to express the protein in BL-21 cells. The optimum expression time and temperature for this protein in LB/kanamycin media was determined to be 3 hours at 37°C. At this time point the cells were pelleted, lysed, and sonicated in order to separate the soluble and insoluble fractions. Western blot analysis of these two fractions showed that this protein is only present in the insoluble fraction (Figure 18). Unfortunately, proteins that are present in the insoluble fraction can only be purified under denaturing conditions. However, this method is not ideal for proteins

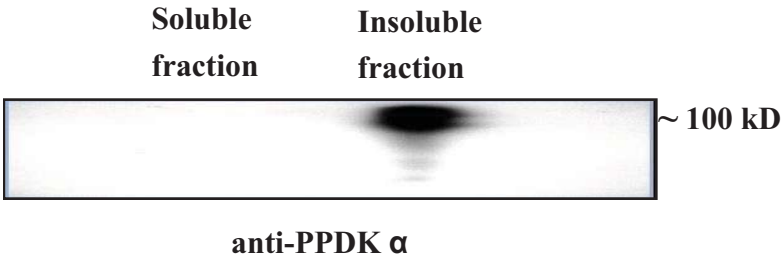

Figure 3.3: Western blot of PPDK/pET28a expressed in BL-21 cells. BL-21 cells induced to express PPDK/pET28a were pelleted lysed and sonicated and the resulting fractions were separated by centrifugation and ran in an SDS-PAGE. Recombinant PPDK was only detected in the insoluble fraction.

that are intended to be used in enzymatic assays as well as crystallography studies due to the potential loss of enzymatic activity as well as the potential for protein misfolding. In order to produce a recombinant protein that is more similar to that in the parasite, we decided to use a yeast expression system known as PichiaPink (Invitrogen). The use of this expression system is currently in progress.

3.3.3 Expression of $PPDK_{Lm}$

As an alternate approach we decided to clone, express, and purify recombinant PPDK from *L. major*. After successfully cloning $PPDK_{Lm}$ into pRSETa we were able to express the protein in BL-21 cells. The optimum expression time and temperature for this protein in LB/amp media was determined to be 4 hours at 30°C. At this time point the cells were pelleted, lysed, and sonicated in order to separate the soluble and insoluble fractions. Western blot analysis of these two fractions showed that this protein is present in the both fractions (Figure 3.4A). The soluble fraction was then collected for

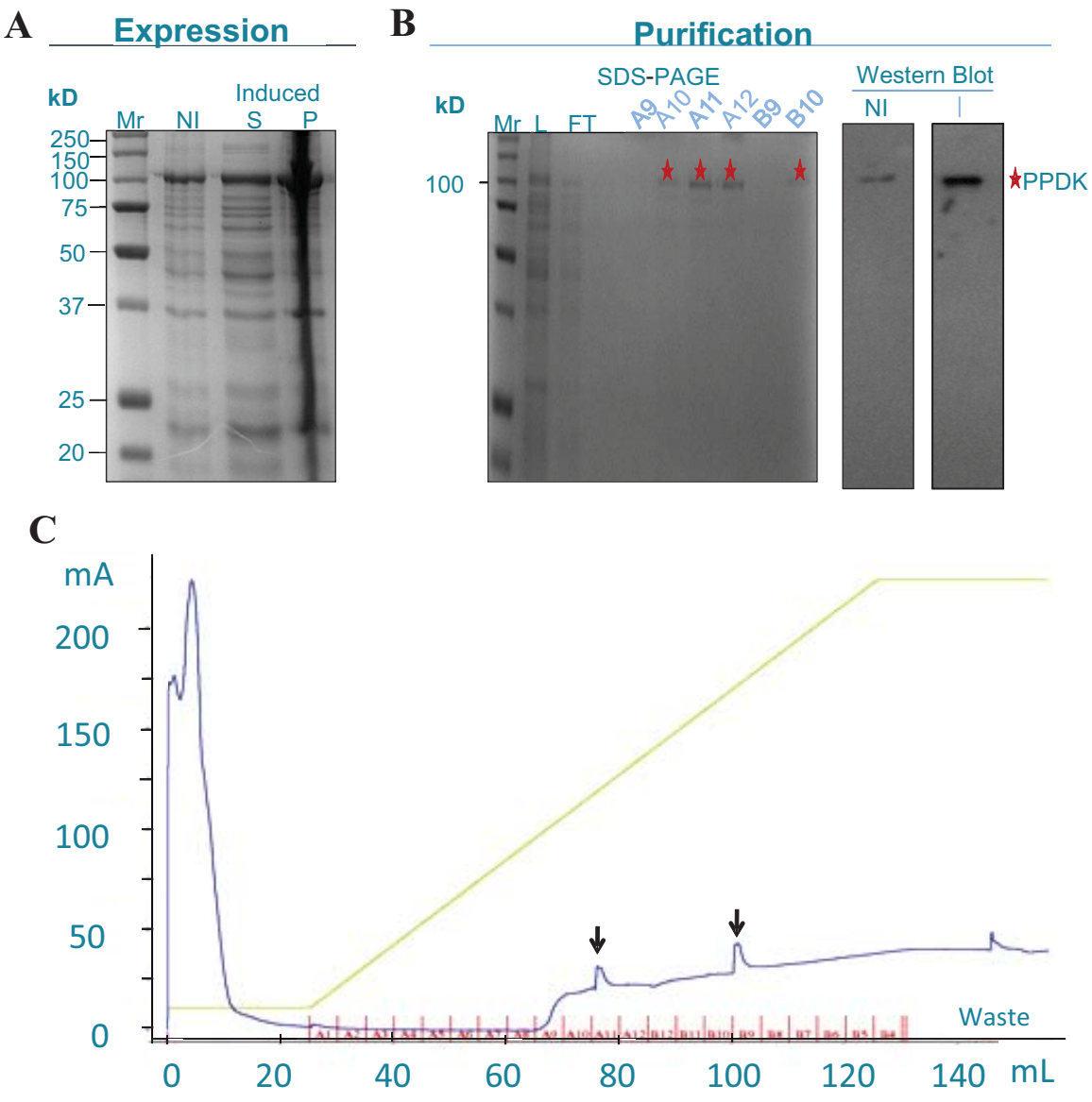

Figure 3.4. (A) Expression of $PPDK_{Lm}$ in non-induced, soluble fraction, and insoluble fractions. (B) Purity of recombinant $PPDK_{Lm}$ was verified by SDS-PAGE and Western blot, as fractions A10, A11 and A12 indicate in Figure 19B and 19C. (C) Chromatogram showing Fast Protein Liquid Chromatography (FPLC) analysis. Peaks indicate presence of a protein in fractions A11 and B9 in which fraction A11 was determined to be $PPDK_{Lm}$.

analysis with FPLC. The soluble fraction was loaded into a HisTrap column and protein fractions were separated using FPLC. The chromatogram in Figure 3.4C above indicates that there is a protein present primarily in fractions A11 and B9. SDS-PAGE analysis confirmed that the protein in fraction A11 is $PPDK_{Lm}$ (Figure 3.4B). Experiments are in progress in order to purify higher amounts of recombinant $PPDK_{Lm}$ that will be used in enzymatic assays.

3.3.4 Analysis of PPDK inhibitors library

The first PPDK inhibitors library generated and sent to our lab by Enamine contained 222 compounds. In order to test the activity and/or toxicity of these compounds against parasites and mammalian cells we conducted viability assays on *L. major* promastigotes and Hs27 human fibroblasts as described previously. The compound library was tested at a final concentration of 50 μM and 5 μM. When tested at 50 μM, 93 compounds showed the ability to inhibit the survival of *L. major* by 50% or more, while only 9 compounds met this criterion at 5 μM. Out the 93 compounds tested positive at 50 μM, 61 compounds exhibited a 50% or greater survivability in Hs27 fibroblasts, while seven of the nine compounds met this criterion at 5 μM (Table 3.1).

Table 3.1: Summary of PPDK inhibitors library analysis in *L. major* promastigotes and Hs27 fibroblasts

No. of Compounds	**222**
< 50% survival of *L.major* at 50 μM	93

< 50% survival of *L.major* at 5 μM	9
> 50% survival of Hs27 at 50 μM	180
> 50% survival of Hs27 at 5 μM	219
Met both criteria at 50 μM	**61**
Met both criteria at 5 μM	**7**

Although only seven of the 222 compounds show potential in the low micromolar range it is still in our interest to conduct further tests on the 61 compounds meeting our criteria at 50 μM as well. Currently used treatment options such as benznidazole to treat Chagas' disease have an LD_{50} that remains in the high micromolar range; therefore, we do not want to rule out any possibilities.

3.3.5 Future Work

The entire compound library will screened against *T. cruzi* epimastigotes at the same concentrations. Also, all of the compounds that met our criteria will be screened at various concentrations to determine the precise difference in the LD_{50} of the parasites as well as in several mammalian cell lines. The most promising compounds will be tested in infectivity assays and possibly *in vivo*. Also, the entire library will be tested in a PPDK enzymatic assay once the recombinant PPDK protein is obtained.

3.4 Discussion

Leishmaniasis and Chagas' disease are both neglected diseases that have caused a great deal of suffering worldwide. The limited amount of treatment options against these diseases as well as the toxicity of these treatment options have compounded the fact that there is an urgent need for new compounds to be developed to treat these parasitoses. In this study, we respond to

this issue using two efficient methods commonly used in drug discovery; 1) High-throughput drug screening of compound libraries synthesized for their biological selectivity and potential therapeutic use and 2) Characterization and validation of an enzyme that is unique to trypanosomatids as a chemotherapeutic target.

A potential chemotherapeutic target in *T. cruzi* and *L. major* is pyruvate phosphate dikinase (PPDK). PPDK is a unique enzyme to trypanosomatids and its role within the glycosome is potentially vital but still not completely understood. The validation of a drug target is an important step in the development of new drugs which includes demonstrating the essentiality of a putative target for the organism. Therefore, we will create a $PPDK_{TC}$ null mutant strain and perform infectivity and viability assays once attained. We expect to see a reduction in the viability and infectivity of the parasite without the presence of this enzyme.

In order to better understand the structure and function of PPDK, experiments generating recombinant PPDK from *T. cruzi* and *L. major* are in progress. The recombinant enzyme will be used to test inhibitors in enzymatic assays for specificity and also may be used for future crystallography experiments. Understanding the substrate specificity of this enzyme could lead to the design of new and better inhibitors against *T. cruzi* and *L. major*. Potential PPDK inhibitors are currently being tested against *L. major* promastigotes and *T. cruzi* epimastigotes. Our first PPDK inhibitors library of 222 compounds made in collaboration with Enamine was tested against *L. major* and Hs27 human fibroblasts. Remarkably, 93 compounds inhibited the survival of the promastigotes by 50% or greater and 61 out the 93 were relatively non-toxic to the mammalian cells at 50 μM. These initial results are very promising and indicate that PPDK may be an essential enzyme for these parasites if the target of these inhibitors is indeed PPDK as predicted. We will be able to determine how specific any of these inhibitors are once the

recombinant PPDK is attained. Overall, we hope to acquire novel knowledge of the parasite to be able to produce effective therapy to alleviate the deleterious effects of Chagas' disease and leishmaniasis.

In conclusion, these experiments provide promising results that may potentially lead to the development of new chemotherapeutic drugs to treat parasitic diseases that are in dire need of new treatment options.

References

1. WHO, *Report of the consultative meeting on Cutaneous Leishmaniasis*. 2007.

2. Alvar J, et al. (2008) The relationship between leishmaniasis and AIDS: The second 10 years. *Clin Microbiol* Rev 21:334–359.

3. Guerin, P. J. 2002. Visceral leishmaniasis: current status of control, diagnosis, and treatment, and a proposed research and development agenda. *Infectious Diseases* Vol 2: 494-501

4. Spread of Disease Tied to U.S. Combat Deployments – Stateside doctors are left grappling". The Boston Globe. John Donnelly. May 7, 2007. Feb. 23 2009. <http://www.boston.com/news/nation/articles/2007/05/07/spread_of_disease_tied_to_us_combat_deployments/>

5. WHO, *Control of Chagas disease.* World Health Organization Technical Reports Series, 2002. 905: p. 24-28.

6. Pintado V, Lopez-Velez R. HIV-associated visceral leishmaniasis. *Clin Microbiol Infect* 2001; 7: 291–300

7. Kima, P. E. 2007. The amastigote forms of Leishmania are experts at exploiting host cell processes to establish infection and persist. *Int. J. Parasitol*. 37: 1087–1096.

8. Parasites and Health. Life Cycle [Leishmaniasis is transmitted by the bite of infected female phlebotomine sandflies]. Digital image. Www.dpd.cdc.gov. Center of Disease Control. 20 Oct. 2008

9. Parasites and Health. Life Cycle [Leishmaniasis is transmitted by the bite of infected female phlebotomine sandflies]. Digital image. Www.dpd.cdc.gov. Center of Disease Control. 20 Oct. 2008 <http://www.dpd.cdc.gov/dpdx/html/frames/g-l/leishmaniasis/body_leishmaniasis_page1.htm>

10. McPhee S. J., Papadakis M. A., 2011. Current Medical Diagnosis and Treatment. *Mcgraw Lange*. p1424-1426.

11. Berman J. *et al*. Oral Miltefosine for Indian Visceral Leishmaniasis. 2002. *New England Journal of Medicine*. Vol 347. No. 22.

12. Germ´an H. Fontanellaa, Kristof De Vusserb, Wouter Laroyb, Lucas Daurelioa, Ana L´ıa Nocitoc, Silvia Revelli, Roland Contrerasb. (2008) Immunization with an engineered mutant *trans*-sialidase highly protects mice from experimental *Trypanosoma cruzi* infection: A vaccine candidate. *Vaccine.* 26, 2322—2334.

13. WHO, *TDR strategic direction for research: Chagas disease.* Available at <http://www.who.int/tdr/diseases/chagas/files/direction.pdf>, 2002.

14. Barrett, M.P., et al., *The trypanosomiases.* Lancet, 2003. 362(9394): p. 1469-80.

15. CDC, *Parasites - American Trypanosomiasis*. 2010. <http://www.cdc.gov/parasites/chagas/epi.html>

16. Engman, D.M. and J.S. Leon, Pathogenesis of Chagas heart disease: role of autoimmunity. *Acta Trop*, 2002. 81(2): p. 123-32

17. Tyler, K.M. and D.M. Engman, The life cycle of Trypanosoma cruzi revisited. *Int J Parasitol*, 2001. 31(5-6): p. 472-81.

18. Rodriques Coura, J. and S.L. de Castro, *A critical review on Chagas disease chemotherapy.* Mem Inst Oswaldo Cruz, 2002. 97(1): p. 3-24.

19. Murta, S.M., et al., Molecular characterization of susceptible and naturally resistant strains of *Trypanosoma cruzi* to benznidazole and nifurtimox. *Mol Biochem Parasitol*, 1998. 93(2): p. 203-14

20. Croft, S.L., M.P. Barrett, and J.A. Urbina, Chemotherapy of trypanosomiases and leishmaniasis. *Trends Parasitol*, 2005. 21(11): p. 508-12

21. Tanowitz, H.B., et al., *Chagas' disease.* Clin Microbiol Rev, 1992. 5(4): p. 400-19

22. Wilkinson, S.R. and J.M. Kelly, Trypanocidal drugs: mechanisms, resistance and new targets. *Expert Rev Mol Med, 2009.* 11: p. e31.

23. Davioud-Charvet, E., Krauth-Siegel, L., Salmon-Chemin, L., 2- and 3-Substituted 1,4-Naphthoquinone Derivatives as Subversive Substrates of Trypanothione Reductase and Lipoamide Dehydrogenase from *Trypanosoma cruzi*: Synthesis and Correlation between Redox Cycling Activities and *In Vitro* Cytotoxicity. *J. Med. Chem*. 2001, 44, 548-565

24. Fairlamb, A.J., Blackburn, P., Ulrich, P., Chait, B.T., and Cerami, A. (1985). Trypanothione: a novel bis(glutathionyl)spermidine cofactor for glutathione reductase in trypanosomatids. Science *227*, 1485-1487.

25. Krauth-Siegel, L., Meiering, S. K., Schmidt, H., The Parasite-Specific Trypanothione Metabolism of Trypanosoma and Leishmania. 2003 *Biol. Chem.*, Vol. 384, pp. 539-49.

26. Boitz, J.M., Yates, P.A., Kline, C., Gaur, U., Wilson, M.E., Ullman, B., Roberts, S.C. *Leishmania donovani* ornithine decarboxylase is indispensable for parasite survival in the mammalian host. *Infect Immun*. 2009 Feb;77(2):756-63

27. Williams, C. H., Jr. In Chemistry and Biochemistry of Flavoenzymes; Muller, F., Ed.; CRC Press: Boca Raton, FL, 1992; Vol. III

28. Gutierrez-Correa, J., *Trypanosoma cruzi* dihydrolipoamide dehydrogenase as target of reactive metabolites generated by cytochrome c/hydrogen peroxide (or linoleic acid hydroperoxide)/phenol systems. *Free Radical Research,* November 2010; 44(11): 1345–1358

29. Tomas, A. M., Castro, H., *Leishmania infantum*: Provision of reducing equivalents to the mitochondrial tryparedoxin/tryparedoxin peroxidase system. *Experimental Parasitology*. 120 (2008) 421–423

30. Maldonado, R. A., Ramos, E. I., 2,3-Diphenyl-1,4-Naphthoquinone: A potential chemotherapeutic agent against *Trypanosoma cruzi*. *Am. J. Parasitol.,* 95(2), 2009, pp. 461–466

31. Klinkert, M. Q., Heussler, V., The Use of Anticancer in Antiparasitic Chemotherapy. *Mini Reviews Med. Chem.* 2006. 6: (2) 131-143 (13).

32. Pati, H. N., Das, U., Sharma, R. K., Dimmock, J. R., Cytoxic Thiol Alkylators. *Mini Reviews Med. Chem.* 2007. 7: 131-139.

33. Dimmock, J. R., Pati, J. N., Das, U., Cytotoxic 3,5-bis(benzylidene)piperidin-4-ones and *N*-acyl analogs displaying selective toxicity for malignant cells. *Eur. J Med. Chem.* 43. (2008) 1-7

34. Hannaert, V., Bringaud, F., Opperdoes, F. R., Michels, P., Evolution of energy metabolism and its compartmentation in Kinetoplastida*. Kinetoplastid Biology and Disease* 2003, 2:11

35. Concepcion, J.L., Acosta, H., Dubourdieu, M., Quinones, W., Caceres, A., Bringaud, F., (2004) Pyruvate phosphate dikinase and pyrophosphate metabolism in the glycosome of *Trypanosoma cruzi* epimastigotes. *Comparative Biochemistry and Physiology*. 138. 347-356

36. Urbina JA, Moreno B, Vierkotter S, Oldfield E, Payares G, Sanoja C, Baliey BN, Yan W, Scott DA, Moreno SNJ, Docampo R. *Trypanosoma cruzi* contains major pyrophosphate stores, and its growth in vitro and in vivo is blocked by pyrophosphate analogs. *J Biol Chem* 1999;273;22151-8

37. Rosa A. Maldonado, Alan H. Fairlamb. (2000) Cloning of a pyruvate phosphate dikinase form *Trypanosoma cruzi*. *Molecular and Biochemical Parasitology*. 112 (2001) 183-191.

38. Dimmock, J.R., K.K. Sidhu, M. Chen, R.S. Reid, T.M. Allen, G.Y. Kao, G. A.Truitt, *Evaluation of some Mannich bases of cycloalkanones and related compounds for cytotoxic activity.* European Journal of Medicinal Chemistry, 1993. 28: p. 313-322.

39. Das, S., et al., *Bis[3,5-bis(benzylidene)-4-oxo-1-piperidinyl]amides: a novel class of potent cytotoxins.* ChemMedChem, 2011. 6(10): p. 1892-9.

40. Andrews, N.W. and W. Colli, *Adhesion and interiorization of Trypanosoma cruzi in mammalian cells.* Journal of Protozoology, 1982. 29(2): p. 264-9.

41. Camargo, E.P., *Growth And Differentiation In Trypanosoma Cruzi. I. Origin Of Metacyclic Trypanosomes In Liquid Media.* Rev Inst Med Trop Sao Paulo, 1964. 12: p. 93-100.

42. Thalhofer, C.J., et al., *In vivo imaging of transgenic Leishmania parasites in a live host.* J Vis Exp, 2010(41).

43. Capul, A.A., et al., *Comparisons of mutants lacking the Golgi UDP-galactose or GDP-mannose transporters establish that phosphoglycans are important for promastigote but not amastigote virulence in Leishmania major.* Infect Immun, 2007. 75(9): p. 4629-37.

44. Martinez, A., et al., *Searching for new chemotherapies for tropical diseases: ruthenium-clotrimazole complexes display high in vitro activity against Leishmania major and Trypanosoma cruzi and low toxicity toward normal mammalian cells.* J Med Chem, 2012. 55(8): p. 3867-77.

45. Lara, D., Feng, Y., Bader, J., Savage, P.B., Maldonado, R.A., *Anti-trypanosomatid activity of ceraginins.* Journal of Parasitology, 2010. 96(3): p. *In press*.

46. Nohara, L.L., et al., *High-content imaging for automated determination of host-cell infection rate by the intracellular parasite Trypanosoma cruzi.* Parasitol Int, 2010. 59(4): p. 565-70.

47. Lonardoni, M.V., M. Russo, and S. Jancar, *Essential role of platelet-activating factor in control of Leishmania (Leishmania) amazonensis infection.* Infect Immun, 2000. 68(11): p. 6355-61.

48. Agarwal, C., R.P. Singh, and R. Agarwal, *Grape seed extract induces apoptotic death of human prostate carcinoma DU145 cells via caspases activation accompanied by dissipation of mitochondrial membrane potential and cytochrome c release.* Carcinogenesis, 2002. 23(11): p. 1869-76.

49. Pati, H.N., et al., *Cytotoxic thiol alkylators.* Mini Rev Med Chem, 2007. 7(2): p. 131-9.

50. Weingärtner A., Kemmer G., Müller F.D., Zampieri R.A., Gonzaga dos Santos M., et al. (2012) *Leishmania Promastigotes Lack Phosphatidylserine but Bind Annexin V upon Permeabilization or Miltefosine Treatment*. PLoS ONE 7(8): e42070. doi:10.1371/journal.pone.0042070

51. Capul, A.A., T. Barron, D. E. Dobson, S. J. Turco, and S. M. Beverley (2007), *Two functionally divergent UDP-Gal nucleotide-sugar transporters participate in phosphoglycan synthesis in Leishmania major.* J. Biological Chemistry 282: 14006-14017.

52. Thalhofer, C.J., J. W. Graff, L. Love-Homan, S. M. Hickerson, N. Craft, S. M. Beverley and M. E. Wilson (2010), *In vivo imaging of transgenic Leishmania parasites in a live host*. Journal of Visual Experimentation. 41: pii: 1980

53. Merdan, T., J. Kopecek, and T. Kissel, *Prospects for cationic polymers in gene and oligonucleotide therapy against cancer.* Adv Drug Deliv Rev, 2002. 54(5): p. 715-58.

54. Halliwell, B. and J.M. Gutteridge, *Role of free radicals and catalytic metal ions in human disease: an overview.* Methods Enzymol, 1990. 186: p. 1-85.

55. Klinkert, M.Q. and V. Heussler, *The use of anticancer drugs in antiparasitic chemotherapy.* Mini Rev Med Chem, 2006. **6**(2): p. 131-43.

56. Krauth-Siegel, R.L., E.M. Jacoby, and R.H. Schirmer, *Trypanothione and N1-glutathionylspermidine: isolation and determination.* Methods Enzymol, 1995. 251: p. 287-94.

57. O'Sullivan S., Sheehan D., Protein Purification Protocols - Fast Protein Liquid Chromatography. *Methods in Molecular Biology*. 2004. Vol. 244. p253-258.

58. Tovar, J., *et al*., Evidence that trypanothione reductase is an essential enzyme in leishmania by targeted replacedment of the tryA gene locus. *Mol. Microbiol.*, 1998. 29(2): p. 654-60.

59. Klinkert M., Q., Heussler V., The Use of Anticancer Drugs in Antiparasitic Chemotherapy. *Mini-Reviews in Medicinal Chemistry*, Volume 6 Issue 2, ISSN: 1389-5575 (13) pp.131-143.

60. Singh, R. G., Roop, G., Enhancement of oral bioavailability of lipophilic drugs from SMEDDS. *Int. J. Drug Dev. and Res.* Sep-Dec 2009; 1(1): 10-18.

Vita

Miguel Vasquez earned his Bachelor of Science degree in Microbiology from the University of Texas at El Paso in May of 2008. In the Fall of 2008, he was accepted into the Biology doctoral program.

While pursuing his undergraduate degree, Miguel Vasquez was exposed to different fields of research while working in a couple of research laboratories. In the summer of 2007, he was accepted into the University of Texas Health Science Center at San Antonio undergraduate research program. During this time he was able to conduct pharmacological behavioral research studies in rodents at one of the largest animal research facilities in Texas. Shortly after the summer internship, Miguel was hired as an HHMI undergraduate research assistant at the University of Texas El Paso Border Biomedical Research Center. During this time he was introduced to the field of infectious diseases. He began his research experience with advanced

techniques such as high throughput drug screening and molecular cloning. These experiences really helped to inspire Miguel to pursue an advanced degree in the field of biology.

Miguel Vasquez has been the recipient of numerous honors and awards including the Research Initiative for Scientific Enhancement (RISE) doctoral fellowship. He was also the recipient of three UTEP graduate school research grants and is involved in many professional organizations such as the American Society for Microbiology (ASM).

Miguel Vasquez has presented his research at many outstanding research conferences such as the Keystone Symposium for Drug Discovery in 2012 and the Kinetoplastid Molecular Cell Biology in 2009 along with many others.

Miguel Vasquez's dissertation entitled, "Identification of chemotherapeutic agents against leishmaniasis and Chagas' disease," was supervised by Dr. Rosa A. Maldonado. This project involved using advanced techniques such as high throughput drug screening, high content imaging, and the use of animal models.

After earning his Ph.D. in Biological Science, Miguel plans to work in the field of industry. There are no limits to what he may do as an experienced researcher and scientist.

Permanent address: 5651 West Valley Circle

El Paso, TX 79932

This thesis/dissertation was typed by Miguel A. Vasquez